European Journal of Medicinal Chemistry 296 (2025) 117860

Contents lists available at ScienceDirect

European Journal of Medicinal Chemistry

journal homepage: www.elsevier.com/locate/ejmech

Research paper

Bacterial cytidine deaminases as versatile activators of fluoropyrimidine nucleoside prodrugs

Viktorija Preitakaitė [a,*], Arūnas Kazlauskas [b], Agota Aučynaitė [a], Kamilė Butkutė [a], Ringailė Lapinskaitė [a,c], Nina Urbelienė [a], Audrius Laurynėnas [a], Rolandas Meškys [a]

[a] Department of Molecular Microbiology and Biotechnology, Institute of Biochemistry, Life Sciences Center, Vilnius University, 7 Saulėtekio Ave, LT-10257, Vilnius, Lithuania
[b] Laboratory of Molecular Neurooncology, Neuroscience Institute, Lithuanian University of Health Sciences, 2 Eivenių Str., LT-50161, Kaunas, Lithuania
[c] Department of Organic Chemistry, Center for Physical Sciences and Technology, 7 Akademijos Str., LT-08412, Vilnius, Lithuania

ARTICLE INFO

Keywords:
Cytidine deaminases
5-Fluoropyrimidine nucleosides
Enzyme-prodrug therapy

ABSTRACT

A platform for modification of 5-fluoropyrimidine nucleosides as potential prodrugs has been developed utilizing bacterial-derived cytidine deaminases (CDAs) for activation. It has been demonstrated that CDA_EH, CDA_F14, and CDA_Lsp effectively convert 5-fluoropyrimidine analogs into 5-fluoro-(2′-deoxy)uridine exhibiting cytotoxic effects. Prodrug activation, leading to reduced viability in CDA-expressing cells, has been observed in HCT116, MCF7, and U87MG cancer cell lines. This framework allows the evaluation of various N^4-acyl/alkyl-5-fluorocytidines, 4-alkylthio-5-fluorouridines, 4-alkoxy-5-fluoro- and 4-alkoxy-5-fluoro-2′-deoxyuridines for their potential use in enzyme-prodrug therapy. Overall, the developed platform provides valuable guidance on selecting both enzyme and prodrug components for the development of effective enzyme-prodrug strategies.

1. Introduction

Prodrugs are, by definition, precursors or derivatives of therapeutically active compounds that undergo bioconversion into their active form within the body, either through spontaneous processes, such as hydrolytic degradation or via biocatalytic mechanisms. The main goal of prodrug design is to mask undesirable drug properties, such as poor water or lipid membrane solubility, low target selectivity, chemical instability, presystemic metabolism, or toxicity [1]. The development of prodrugs primarily focuses on the structural features of the parent drug molecule, particularly the availability of chemical functionalities that enable masking the drug's pharmacodynamic activity, often by attaching a modifying group. Another crucial aspect in the prodrug development process is the bioconversion mechanisms involved in drug release, which, although spontaneous in some cases, are predominantly carried out through enzymatic processes [2,3]. Prodrug technology has gained significant attention recently for its ability to improve the therapeutic efficacy of drugs, as demonstrated by the growing number of newly approved prodrug-based pharmaceuticals [4]. However, there is still a notable gap in research to fully establish prodrugs as a stable and reliable component of modern therapy.

Enzyme-prodrug therapy (EPT) is a rapidly progressing field with great potential for offering advanced drug delivery options. Prodrugs for EPT are designed to undergo bioconversion by a specific enzyme placed in a targeted location within the body, ensuring that activation occurs only at the enzyme's site of action [5,6]. The most widely researched approach in EPT, with numerous clinical trials underway, is gene-directed enzyme-prodrug therapy (GDEPT), also known as suicide gene therapy [7]. GDEPT involves three key components: the prodrug to be activated, the enzyme (usually nonhuman) responsible for activation, and the delivery system for the corresponding gene [8]. In GDEPT, the enzyme needed for prodrug modification is expressed exclusively in the target cells, with activation almost entirely relying on intracellular processes. The precise predisposition to target cells increases the therapeutic index of prodrugs, making GDEPT particularly promising for cancer treatment [9].

One of the most extensively researched GDEPT systems for cancer therapy is the combination of cytosine deaminase (CD) and the prodrug 5-fluorocytosine (5-FC). CD catalyzes cytosine conversion into uracil, a process found in many bacteria and fungi but absent in mammalian cells. The low-toxicity pyrimidine prodrug 5-FC is converted by CD into the highly toxic 5-fluorouracil (5-FU), which is subsequently processed into

* Corresponding author.
E-mail address: viktorija.preitakaite@gmc.vu.lt (V. Preitakaitė).

https://doi.org/10.1016/j.ejmech.2025.117860
Received 1 May 2025; Received in revised form 28 May 2025; Accepted 9 June 2025
Available online 10 June 2025

5-fluorouridine and 5-fluoro-2′-deoxyuridine [10]. These metabolites are further processed by cellular enzymes into potent pyrimidine antimetabolites (5-fluoro-2′-deoxyuridine 5′-monophosphate, 5-fluoro-2′-deoxyuridine 5′-triphosphate, and 5-fluorouridine 5′-triphosphate), which induce cell death through three distinct mechanisms: inhibiting thymidylate synthase, forming 5-FU DNA, and 5-FU RNA complexes [11,12]. Furthermore, recent findings suggest that ribosome collisions and defects in ribosomal RNA processing drive 5-FU toxicity, potentially through RNA writer inhibition [13]. The CD/5-FC exploits the cytotoxic effects of 5-FU, which can induce growth inhibition and apoptotic cell death in various solid tumors, including gastric [14], head and neck [15], colon [16], prostate cancer [17], melanoma [18], and glioma [19].

Several clinical trials have been conducted using the CD/5-FC with limited success [20]. This is likely due to several limitations that hinder its therapeutic effectiveness. A primary issue is the short half-life of 5-FC in the bloodstream, which decreases its availability at the tumor site [21]. Additionally, wild-type CD has poor activity against 5-FC, which hampers the overall therapeutic response [22]. While increasing 5-FC doses could address this, it also leads to an increased probability of side effects. A significant concern is systemic toxicity, as bacteria in the gut can produce CD and convert 5-FC to 5-FU at the non-target site, the intestine [23]. Kazlauskas and colleagues have introduced a new strategy involving isocytosine deaminase (ICD) and 5-fluoroisocytosine (5-FIC) with greater potential than the CD/5-FC [24]. ICD specifically converts 5-FIC into 5-FU, with the advantage that gut microbiota are less likely to metabolize 5-FIC. The ICD/5-FIC was reported to increase mice survival rate compared to 5-FU alone and is theorized to reduce the toxic side effects typically associated with the CD/5-FC [24]. A novel GDEPT strategy, extensively investigated by our team [25], involves modified pyrimidine nucleosides as prodrugs, bypassing the need to use nucleobases as prodrugs and convert 5-FU to nucleosides. In this approach, acylated 5-fluorocytidines are activated by bacterial amidohydrolases, leading to the formation of toxic metabolite precursors. The amidohydrolases used in our previous work are relatively small, catalytically efficient, and have a broad substrate spectrum. These enzyme properties are advantageous in GDEPT compared to classically used CD [25]. No active clinical trials are currently underway using GDEPT strategies based on 5-FU and its metabolites, highlighting the need for further development of both the enzyme and prodrug components of GDEPT.

Cytidine deaminases (CDAs) are among the enzymes that show potential for enhancing GDEPT. CDAs catalyze the hydrolytic deamination of cytidine and 2′-deoxycytidine to uridine and 2′-deoxyuridine. Additionally, CDAs play a crucial role in the metabolism of nucleoside analogs, which are extensively utilized as anticancer prodrugs [26]. A well-known example is the 5-fluoropyrimidine carbamate capecitabine, whose conversion to 5-FU is mediated by a cascade of three enzymes, including human CDA [27]. While capecitabine demonstrates improved therapeutic efficacy over 5-FU, several challenges remain, such as prodrug metabolism by the gut microbiota and the variability in human CDA activity between different patients [28–30]. Recent studies by Urbelienė and colleagues have identified several prokaryotic homo-tetrameric CDAs capable of converting S^4-/N^4-/O^4-modified pyrimidine nucleosides, as well as 5-fluoropyrimidines directly into uridine derivatives [31]. These enzymes present advantages over conventional human CDA, as they directly generate toxic metabolites without requiring additional enzymes, such as esterases, and possess a broad substrate spectrum. These characteristics highlight the potential of newly identified CDAs in developing novel enzyme-prodrug strategies for cancer therapy (Fig. 1).

This study examined the ability of prokaryotic CDAs to activate prodrugs based on modified fluorinated nucleosides. In order to identify the potential prodrugs, a select set of substrates was synthesized, including fluorinated N^4-acyl-pyrimidine, 4-alkylthio-pyrimidine, N^4-alkyl-pyrimidine, and 4-alkoxy-pyrimidine nucleosides. As candidate enzymes for prodrug activation, CDA_EH, CDA_F14, and CDA_Lsp were selected, previously shown to possess the broadest substrate spectrum [31]. These CDAs' ability to catalyze the conversion of synthesized substrates were assessed both *in vitro* and in cancer cell lines. The results uncovered new potential enzyme-prodrug systems and established a platform for the development and screening of novel prodrugs.

2. Results

2.1. CDAs target various modified fluorinated pyrimidine nucleosides

A select set of modified fluorinated pyrimidine nucleosides were synthesized to investigate their potential to be used as enzymatically activated prodrugs (Fig. 2). This substrate collection included control toxic compounds (**1**–**3**), N^4-acyl-5-fluorocytidines (**4**–**7**), 4-alkylthio-5-fluorouridines (**8**–**17**) (in both acetylated and deacetylated forms), N^4-alkyl-5-fluorocytidines (**18**–**24**), 4-alkoxy- and 4-aryloxy-5-fluorouridines (**25**–**41**) (in both acetylated and deacetylated forms), and 4-alkoxy-5-fluoro-2′-deoxyuridines (**42**–**49**) (in both acetylated and deacetylated forms).

The synthesized substrates were evaluated for their *in vitro* enzymatic activation into toxic compounds. Three CDAs, namely CDA_EH, CDA_F14, and CDA_Lsp, were selected for this analysis. Based on previously reported findings that these CDAs exhibit a broad substrate spectrum [31], they were hypothesized to activate at least some of the selected modified 5-fluoropyrimidines. Recombinant CDA_EH, CDA_F14, and CDA_Lsp were overexpressed in *E. coli* HMS174Δ*pyrF*Δ*cdd* cells and purified following previously established protocol [31]. It is important to note that the *in vitro* LC-MS analysis was

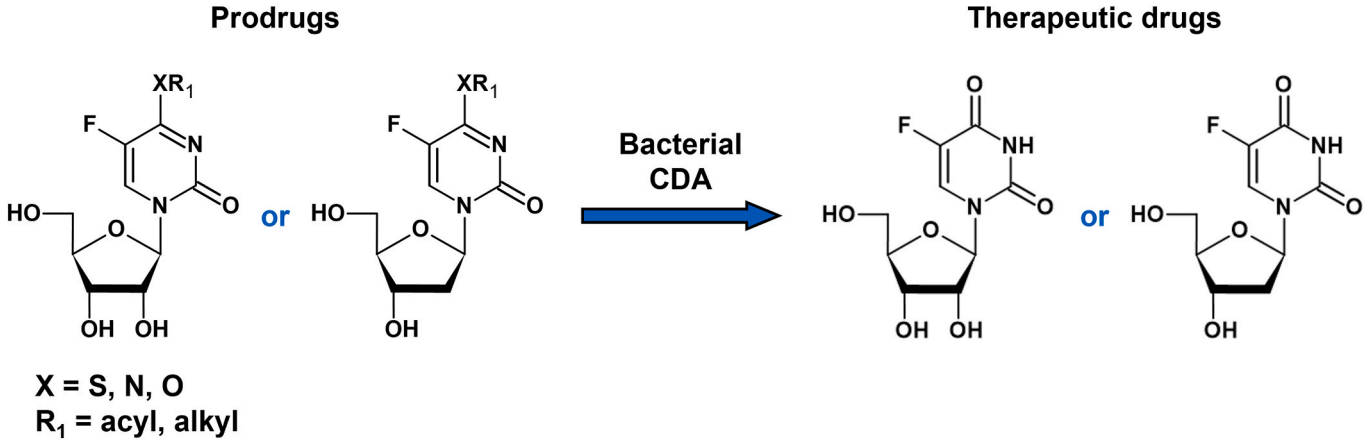

Fig. 1. Graphical representation of bacterial CDA-mediated activation of anticancer prodrugs.

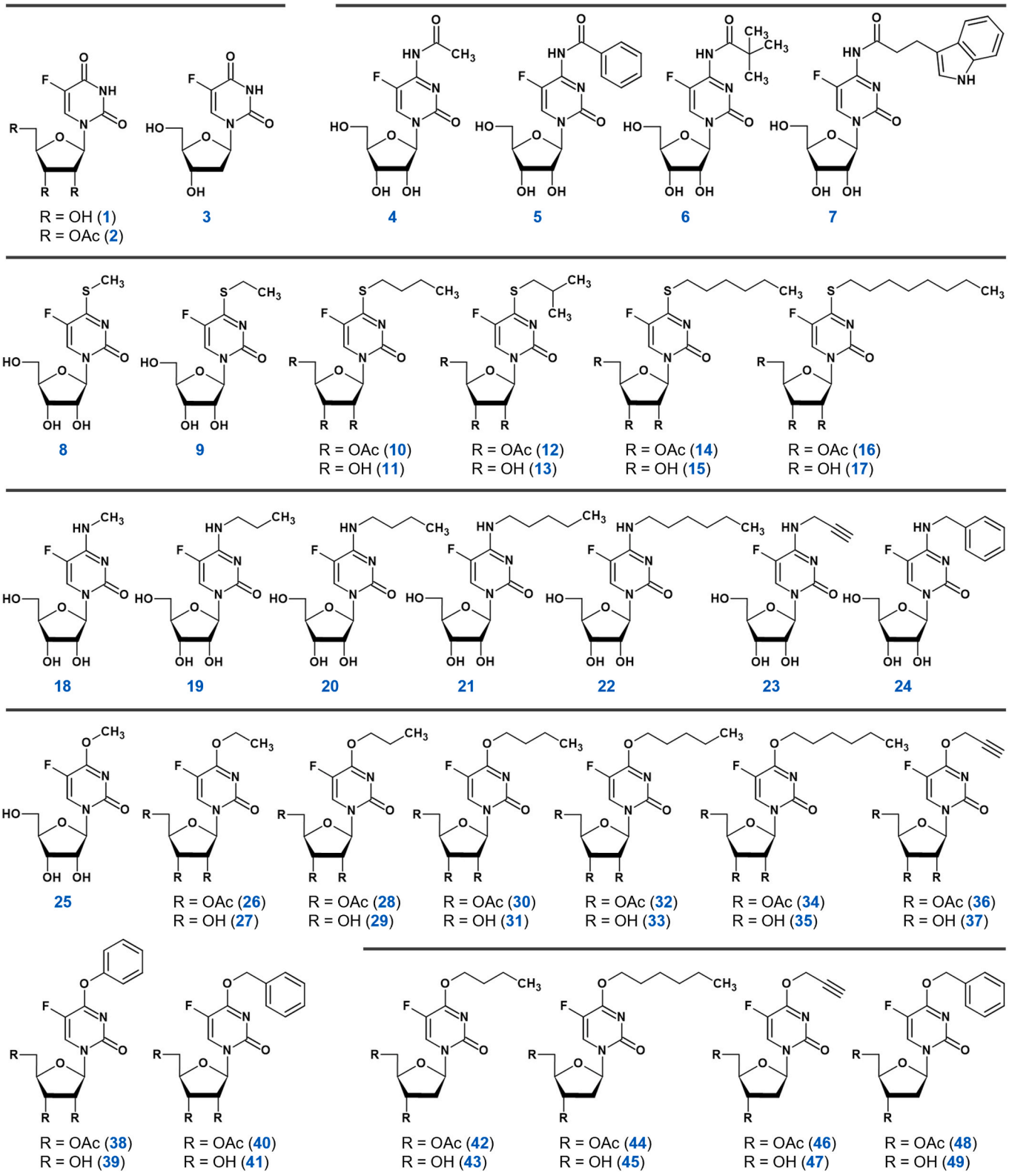

Fig. 2. Structural overview of modified fluorinated pyrimidine nucleosides utilized in this study.

conducted solely to qualitatively confirm enzymatic activity toward the target substrates; a representative chromatogram illustrating this analysis is provided in Fig. S86 (Supplementary Material (SM), Section S3).

No conversion was detected for the acetylated substrates (**10**, **12**, **14**, **16**, **26**, **28**, **32**, **34**, **36**, **38**, **42**, **44**, **46**, **48**), indicating that CDA_EH, CDA_F14, and CDA_Lsp do not accept acetylated compounds as substrates. In contrast, substrates with free ribose moiety (**11**, **13**, **15**, **17**–**24**, **27**, **29**, **33**, **35**, **37**, **39**, **43**, **45**, **47**, **49**) were accepted by the enzymes, with two exceptions: CDA_EH showed only minimal activity towards 5-fluoro-N^4-methylcytidine (**18**), producing only trace amounts of product after 1 h; and CDA_F14 showed no activity towards 5-fluoro-4-octylthiouridine (**17**), with no product formation detected after 1 h.

These findings highlight the ability of the evaluated CDAs to activate 5-fluoropyrimidines with diverse modifications and allow for further exploration of novel enzyme-prodrug systems in cancer cell lines.

2.2. Bacterial CDA_Lsp activates N^4-acyl-fluorocytidines in cancer cell lines

CDA_EH, CDA_F14, and CDA_Lsp efficiently converted 5-fluoropyrimidine analogs *in vitro* (SM, Fig. S86 in Section S3). Therefore, we analyzed the ability of CDAs to activate modified 5-fluoropyrimidines in cancer cells. HCT116 and MCF7 cell lines were engineered to express bacterial CDAs. The genes encoding bacterial CDA_EH, CDA_F14, and CDA_Lsp were individually integrated into the genomes of HCT116 and MCF7 cells via retroviral transduction. Gene expression in generated cell lines was confirmed by real-time PCR (Fig. 3).

Western blot analysis was performed to assess the expression of bacterial CDAs at the protein level. Protein bands corresponding to CDA_EH, CDA_F14, and CDA_Lsp were undetected in the HCT116 and MCF7 cell samples. These results align with our previous findings, where the biosynthesis of bacterial enzymes in eukaryotic cells did not reach the detection threshold of the Western blot method [25]. However, despite the low enzyme expression levels, enzymatic activity was still detectable, and treatment with different prodrugs led to biologically significant viability changes in the cancer cell lines [25]. Therefore, further investigation was undertaken to determine whether the bacterial CDAs could activate modified 5-fluoropyrimidines inside the cancer cells. The activity of CDA_Lsp towards N^4-acyl-5-fluorocytidines (**4**–**7**) was evaluated first. HCT116 and MCF7 cell lines expressing CDA_Lsp were treated with **4**–**7**, with concentration ranges (1–10 μM for HCT116 and 10–100 μM for MCF7) selected based on our previous work [25]. Cell viability was assessed by MTT assay 24 h post-exposure, and results were compared to control cells transduced with a vector lacking the gene insert (Fig. 4).

The viability of HCT116 cells expressing CDA_Lsp was significantly reduced following exposure to all N^4-acyl-5-fluorocytidines tested. Notably, the most pronounced differences in viability between control and the cells expressing CDA_Lsp were observed after treatment with 5 μM and 10 μM concentrations of compounds. These findings suggest CDA_Lsp effectively activates N^4-acyl-5-fluorocytidines within cancer cells, forming a toxic metabolite that reduces cell viability. In contrast, no significant difference in viability was observed between control and CDA_Lsp-expressing MCF7 cells, suggesting a cell line-specific response to N^4-acyl-5-fluorocytidines. Additionally, issues related to the stability of the compounds were noted during this study, which may have influenced the results. These observations underscore the need for further research into modified 5-fluoropyrimidines to develop chemically stable and broadly effective compound variants.

2.3. Bacterial CDA_EH, CDA_F14, and CDA_Lsp activate $S^4/O^4/N^4$-substituted 5-fluoropyrimidines in cancer cell lines

The enzymatic activity of bacterial CDAs in catalyzing the conversion of $S^4/O^4/N^4$-substituted 5-fluoropyrimidines within cancer cells was further examined. HCT116 and MCF7 cell lines expressing bacterial CDA_EH, CDA_F14, and CDA_Lsp were treated with 4-alkylthio-5-fluorouridines (**8**, **9**), N^4-alkyl-5-fluorocytidines (**22**, **23**), and 4-alkoxy-5-fluorouridines (**25**, **27**, **30**, **31**, **41**). Cells were exposed to the target substrates at concentrations of 5 μM, 10 μM, and 100 μM for 48 h, followed by evaluation of cell viability via MTT assay (Fig. 5). Detailed graphs illustrating changes in cell viability are provided in SM (Section S4).

The cell viability results revealed notable variations in the prodrug-activating enzymes and the cell lines. Exposure to 4-methylthio-5-fluorouridine (**8**) at the highest concentration (100 μM) demonstrated a viability decrease of the HCT116 cell line, where more efficient conversion was observed in cells expressing CDA_F14 and CDA_Lsp. In contrast, compound **8** was highly toxic to MCF7 cells, and no significant differences in cell viability were observed between control cells and those expressing the CDAs. Higher concentrations of 4-ethylthio-5-fluorouridine (**9**) effectively reduced the viability of HCT116 cells expressing CDAs, with the CDA_Lsp enzyme showing the most efficient conversion. In MCF7 cells, CDA_EH and CDA_F14 were more effective; however, at higher concentrations compound **9** exhibited toxicity in control cells. The treatment of MCF7 cells with both N^4-hexyl- and N^4-propargyl-5-fluorocytidines (**22** and **23**) displayed differences in cell viability between CDA-expressing and control cells, even at the lowest concentration of 5 μM. Compound **22** was more efficiently activated by CDA_EH, whereas **23** showed greater activation by CDA_F14 and

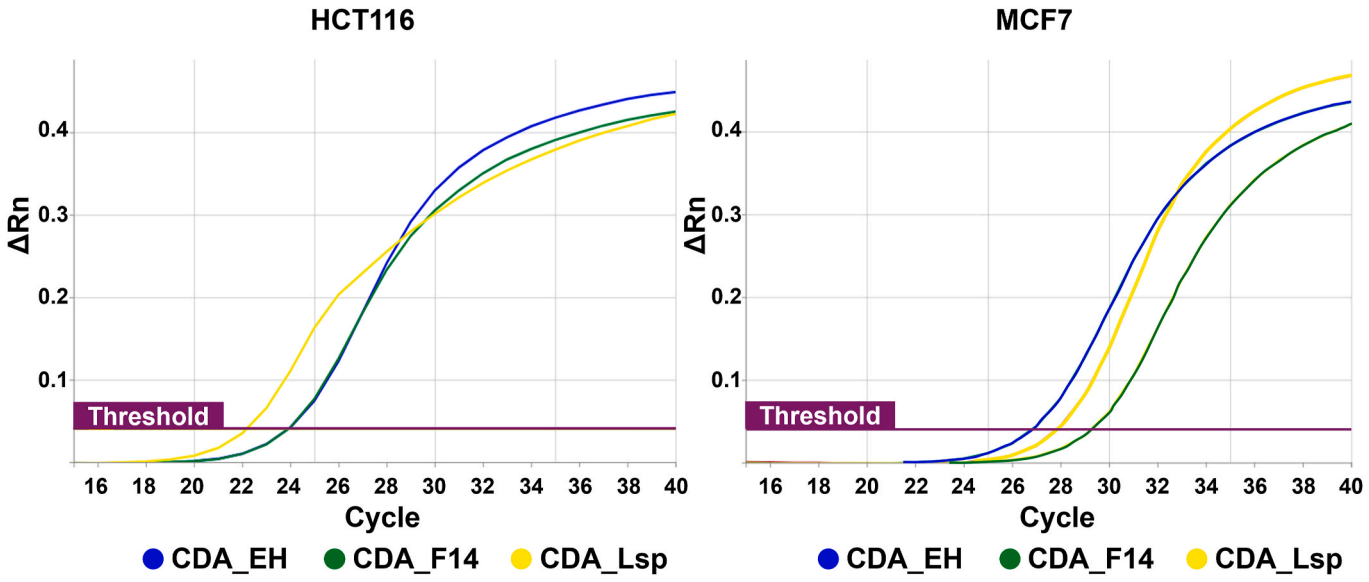

Fig. 3. Confirmation of *cda_eh*, *cda_f14*, and *cda_lsp* expression in HCT116 and MCF7 cells by real-time PCR. Amplification plots for different transduced cell lines displayed (y-axis (ΔRn) – normalized fluorescence of SYBR Green probe, x-axis – PCR cycle number). Exponential increase of fluorescence with values crossing the threshold confirms the presence of *cda_eh*, *cda_f14*, and *cda_lsp* mRNA in the corresponding transduced cell lines. (For interpretation of the references to color in this figure legend, the reader is referred to the Web version of this article.)

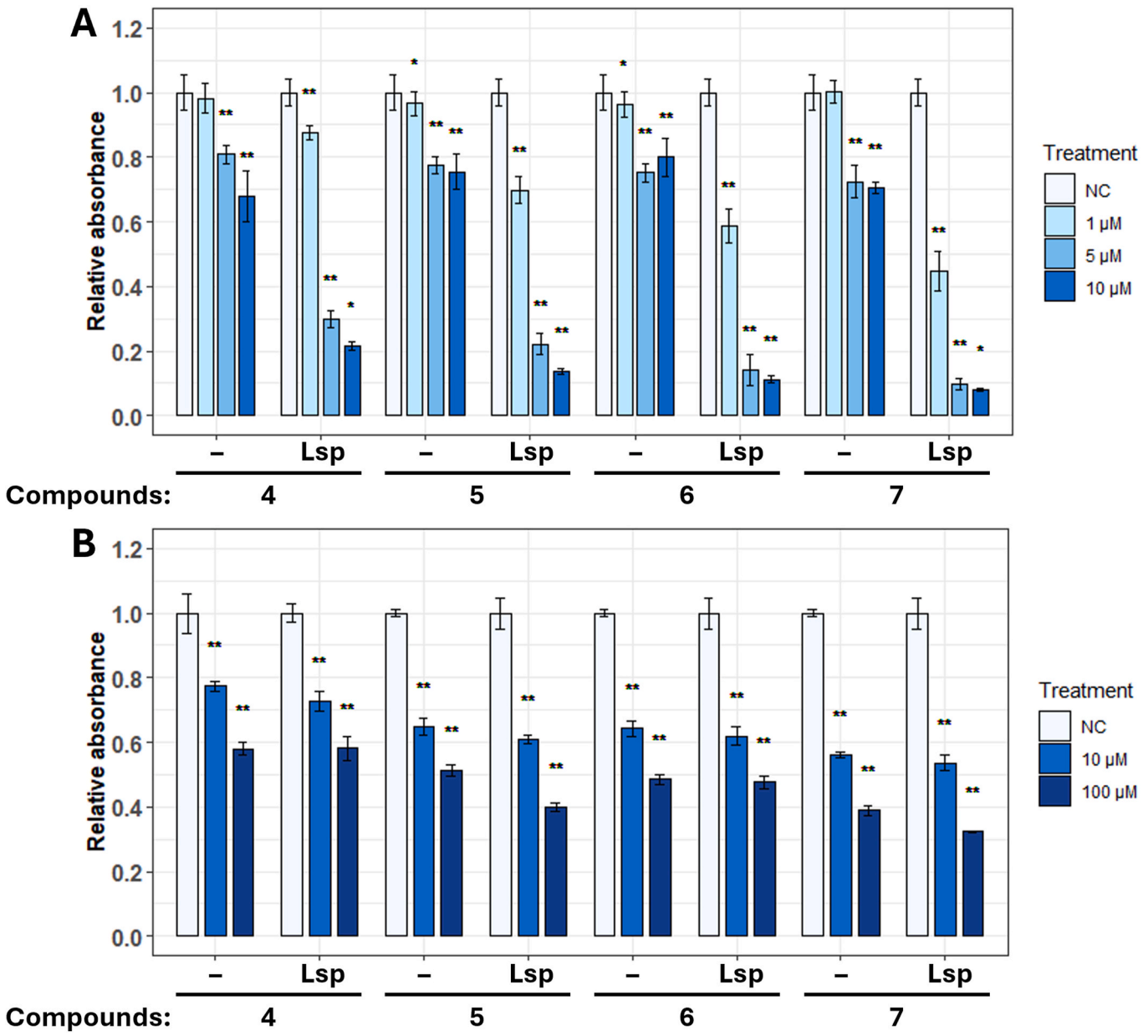

Fig. 4. MTT assay of HCT116 (A) and MCF7 (B) cell lines expressing CDA_Lsp following treatment with compounds **4**–**7**. Cell lines transduced with CDA_Lsp-encoding vector pBABE-CDA_Lsp (designated as Lsp) or control vector pBABE-Puro (designated as symbol –) were exposed to several different concentrations (1–10 μM for HCT116; 10–100 μM for MCF7) of compounds for the 24 h. Statistical significance is indicated by *p*-values, where the symbol * designates $p < 0.05$, whereas the symbol ** designates $p < 0.01$ with respect to untreated cells (negative control (NC)). Each data point represents the mean of eight technical replicates (n = 8).

CDA_Lsp. Unlike **23**, compound **22** did not cause toxicity in control cells, even at a concentration of 100 μM. The 4-alkoxy-5-fluorouridines (**25**, **27**, **30**, **31**, **41**) also produced variable results in cell viability. 4-Methoxy-5-fluorouridine (**25**) was highly toxic to both HCT116 and MCF7 cells, while 4-ethoxy-5-fluorouridine (**27**) significantly reduced cell viability in CDA_EH and CDA_Lsp-expressing HCT116 cells at a concentration of 100 μM. Although 100 μM concentration of **27** was toxic to MCF7 cells, treatment with 10 μM of **27** in CDA_F14 and CDA_Lsp-expressing MCF7 cells significantly reduced cell viability. We also included acetylated derivatives in our analysis to assess the impact of ribose hydroxyl group protection on compound behavior. This approach evaluated whether acetylation enhances chemical stability and reduces cytotoxicity in control cells while enabling activation in CDA-expressing cells via intracellular esterases. 5-Fluoropyrimidines with 4-butoxy group **30** and **31** reduced the viability of CDA_EH-expressing MCF7 cells even at 5 μM concentration, although the conversion of these compounds was less effective in CDA_F14 and CDA_Lsp-expressing cells. Compound **30**, unlike **31**, did not exhibit toxic effects to control cells even at high concentrations. Since **30** is an acetylated derivative of **31**, these results suggest that the acetylated compounds may be better tolerated by the cells while still undergoing conversion in CDA-expressing cell lines. This implies that further research could directly explore using acetylated compounds without removal of protecting group prior to the cell treatment. 4-Benzyloxy-5-fluorouridine (**41**) effectively reduced the viability of CDA_EH-expressing HCT116 cells at concentrations of 5 μM and 10 μM. However, higher concentration was toxic to control cells. 5-Fluorouridines with 4-butylthio, 4-isobutylthio, 4-hexylthio and 4-octylthio substituents (**11**, **13**, **15**, **17**) and 4-phenoxy-5-fluorouridine (**39**) were also tested for their potential activation in the HCT116 cell line expressing bacterial CDA_Lsp. While these compounds

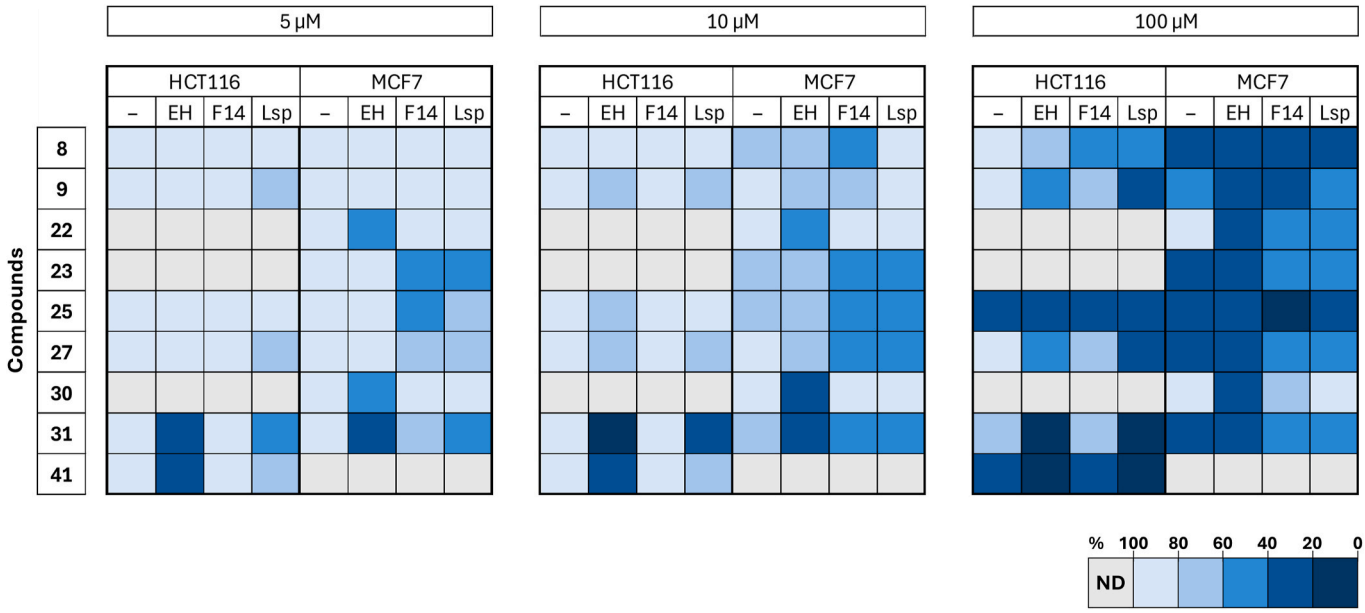

Fig. 5. Graphical representation of viability changes in HCT116 and MCF7 cell lines expressing bacterial CDA_EH, CDA_F14, and CDA_Lsp following exposure to S^4/O^4/N^4-substituted 5-fluoropyrimidines. Cell lines transduced with CDA_EH-encoding vector pBABE-CDA_EH (designated as EH), CDA_F14-encoding vector pBABE-CDA_F14 (designated as F14), CDA_Lsp-encoding vector pBABE-CDA_Lsp (designated as Lsp) or control vector pBABE-Puro (designated as symbol "–") were exposed to 5 μM, 10 μM, and 100 μM concentrations of compounds for 48 h. ND – not determined.

demonstrated chemical stability and had minimal impact on the viability of control cells, no significant differences in cell viability were observed between control and CDA_Lsp-expressing cells (SM, Fig. S87 in Section S4). In summary, bacterial CDA_EH, CDA_F14, and CDA_Lsp were capable of activating select 4-alkylthio-5-fluorouridines, N^4-alkyl-5-fluorocytidines, and 4-alkoxy-5-fluorouridines in HCT116 and MCF7 cancer cells. Although these bacterial CDAs exhibited similar enzymatic activity, cell viability after prodrug treatment varied depending on the specific CDA expressed. Most prodrugs showed higher toxicity to control MCF7 cells than the control HCT116 cells. N^4-alkyl-5-fluorocytidines and 4-alkoxy-5-fluorouridines offered advantages over 4-alkylthio-5-fluorouridines in reducing cell viability at lower concentrations while causing minimal toxicity to control cells. However, the observed differences between the prodrugs within the same groups underscore the importance of evaluating the effects of each compound on cancer cells individually.

2.4. Human-optimized versions of CDA_EH, CDA_F14, and CDA_Lsp provide improved activation of modified 5-fluoropyrimidines in cancer cells

The analysis of bacterial CDAs' ability to activate modified 5-fluoropyrimidines in cancer cell lines yielded mixed results. This variability may be attributed to the limited biosynthesis of bacterial enzymes in eukaryotic cells. Therefore, human codon-optimized variants of CDA_EH, CDA_F14, and CDA_Lsp were developed and integrated into the genomes of HCT116 and MCF7 cells. The expression of the optimized variants in the cell lines, both at the gene and protein levels, was confirmed through real-time PCR (Fig. 6A) and Western blot analysis (Fig. 6B and SM, Fig. S88 in Section S5).

The conversion of modified 5-fluoropyrimidines by human codon-optimized CDAs in cancer cell lines was further examined. HCT116 and MCF7 cells expressing human-optimized CDA_EH, CDA_F14, and CDA_Lsp were exposed to various compounds, including 4-alkylthio-5-fluorouridines (**8**, **9**), N^4-alkyl-5-fluorocytidines (**18**–**24**), 4-alkoxy-5-fluorouridines (**25**, **27**, **28**, **30**, **31**, **32**, **34**, **36**, **40**, **41**), and 4-alkoxy-5-fluoro-2′-deoxyuridines (**42**, **44**, **46**, **48**). Two pairs of 4-alkoxy-5-fluorouridines were evaluated in both acetylated and deacetylated forms (**30** and **31**; **40** and **41**), whereas the remaining compounds were analyzed in either the acetylated or deacetylated form only. Cell viability was assessed using the MTT assay 48 h after exposure (Fig. 7). Detailed graphs illustrating the changes in cell viability are provided in SM (Section S5).

None of the potential prodrugs tested exhibited intrinsic toxicity to HCT116 control cells at a concentration of 5 μM. Only minimal toxicity was observed for N^4-methyl- and N^4-propyl-5-fluorocytidines (**18** and **19**) when exposed to HCT116 control cells at 10 μM. The lowest concentrations of the tested compounds also did not induce toxicity in control MCF7 cells, with the exceptions of **18** and **41** (4-benzyloxy-5-fluorouridine). Although, **18** did not appear to be a suitable prodrug for the HCT116 cells, as no significant difference in viability was observed between control and CDA-expressing cells. In contrast, **41** significantly reduced the viability of HCT116 cells expressing CDA_EH and CDA_Lsp. When comparing the 4-alkylthio-5-fluorouridines, a more pronounced effect on cell viability was observed with 4-ethylthio-substituted uridine **9** than with 4-methylthio group bearing compound **8**. Additionally, **9** activation in human codon-optimized CDA-expressing cells was more efficient than in bacterial CDA-expressing cells (see Fig. 5). N^4-alkyl-5-fluorocytidines demonstrated considerable potential as prodrugs, primarily due to their efficient activation in CDA-expressing cell lines and the minimal toxicity to control cells across a wide range of concentrations. Cytidines with longer alkyl moiety (**20**, **21**, **22**, and **24**) induced significant decreases in viability in CDA-expressing HCT116 cell lines, while all of these, along with N^4-propyl-5-fluorocytidine (**19**), also showed similar effects in CDA-expressing MCF7 cell lines. Notably, compounds **22** and **23** were more efficiently activated in human-optimized CDA-expressing cell lines compared to bacterial CDA-expressing cell lines (see Fig. 5). However, despite codon optimization, differences in cell viability after exposure to prodrugs between CDA_EH, CDA_F14, or CDA_Lsp-expressing cell lines remained, indicating that CDAs exhibited varying preferences for different prodrugs. Most of the 4-alkoxy-5-fluorouridines tested showed potential as candidates for prodrug therapy. Compounds **27**, **30**, **31**, **32**, **34**, and **41** significantly reduced the viability of CDA-expressing HCT116 cells at the lowest concentrations tested, with similar effects observed in MCF7 cell lines for these compounds, as well as compound **25**. Compounds **25**,

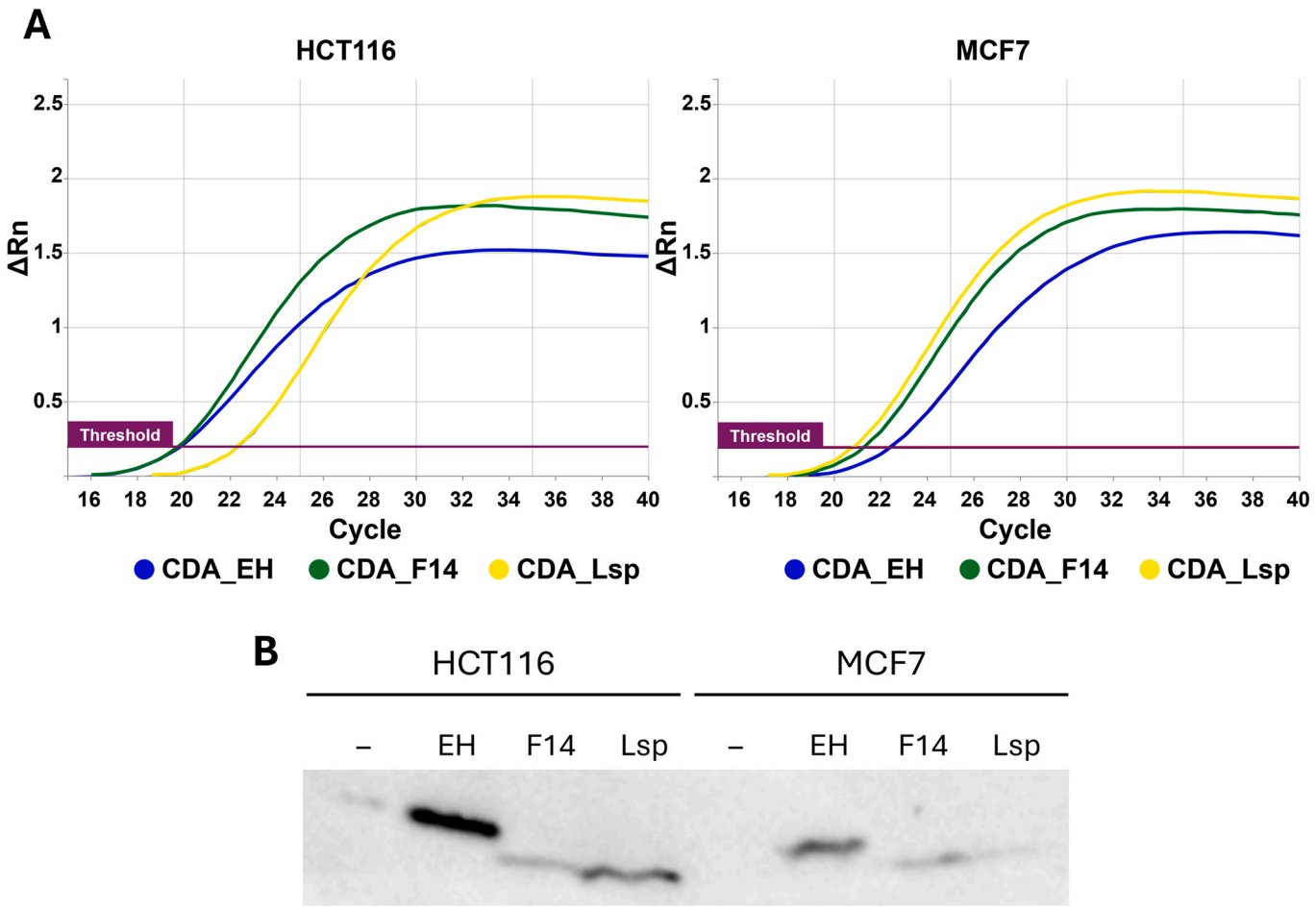

Fig. 6. Expression of human codon-optimized CDA_EH, CDA_F14, and CDA_Lsp in HCT116 and MCF7 cell lines at the gene (A) and protein (B) level. Amplification plots for different transduced cell lines displayed (y-axis (ΔRn) – normalized fluorescence of SYBR Green probe, x-axis – PCR cycle number). Exponential increase of fluorescence with values crossing the threshold confirms the human-optimized version of *cda_eh*, *cda_f14*, and *cda_lsp* mRNA in the corresponding transduced cell lines. Whole-cell extracts of HCT116 and MCF7 cell lines expressing CDA_EH (designated as EH), CDA_F14 (designated as F14), CDA_Lsp (designated as Lsp) or control cells (designated as symbol –) were loaded into a gel and protein bands were detected using antibody against FLAG epitope Tag. (For interpretation of the references to color in this figure legend, the reader is referred to the Web version of this article.)

27, **30**, **31**, and **41** were more efficiently activated in human-optimized CDA-expressing cells than in bacterial CDA-expressing cells (see Fig. 5). The activity of different CDAs towards 4-alkoxy-5-fluorouridines in cancer cells was variable, with the most efficient conversion of prodrugs to toxic metabolites occurring in CDA_EH and CDA_Lsp-expressing cell lines. Acetylated 4-butoxy- and 4-benzyloxy-5-fluorouridines **30** and **40** were better tolerated by control cells at higher concentrations than their deacetylated derivatives, **31** and **41**, respectively. However, **31** and **41** were more effective than **30** and **40** in reducing the viability of CDA-expressing cells at lower concentrations. Therefore, specific experimental design should guide the choice between acetylated and deacetylated compounds for further studies. Treatment of cells with acetylated 4-alkoxy-5-fluoro-2'-deoxyuridines (**42**, **44**, **46**, **48**) produced promising results. They significantly reduced the viability of CDA_EH- and CDA_Lsp-expressing MCF7 cell lines when treated with 5 μM, with similar effects observed for 2'-deoxyuridines **42** and **48** in HCT116 cell lines. A pronounced decrease in the viability of CDA-expressing cells was also noted after exposure to 100 μM concentrations of **42** and **44**, whereas the viability of control cells remained unaffected. In summary, the results highlighted several compounds for further evaluation, demonstrating their potential for prodrug development based on their chemical stability and effectiveness in reducing the viability of cancer cells. The varying substrate preferences of different CDAs were also observed, facilitating the selection of the most appropriate enzyme-prodrug pair for specific applications.

2.5. *CDA_Lsp activates N^4/O^4-substituted fluorinated nucleosides in U87MG human glioblastoma cell line*

Several compounds that effectively reduced the viability of CDA-expressing HCT116 and MCF7 cells were selected for further analysis. The human glioblastoma U87MG cell line was chosen to evaluate the versatility of the CDA-modified 5-fluoropyrimidine enzyme-prodrug system. The gene encoding human codon-optimized CDA_Lsp was integrated into the genome of U87MG cells. The expression of CDA_Lsp in the generated cell line was confirmed through Western blot analysis (SM, Fig. S89 in Section S5). Next, the ability of CDA_Lsp to activate prodrugs within U87MG cells was investigated. For this purpose, N^4-propyl- and N^4-pentyl-5-fluorocytidines (**19**, **21**), and acetylated 4-butoxy-5-fluorouridine **30**, which exhibited high efficacy in earlier experiments, were selected. The CDA_Lsp-expressing U87MG cells were treated with **19**, **21**, and **30** for 72 h, after which cell viability was assessed using the MTT assay (Fig. 8).

The results demonstrated a significant decrease in the viability of CDA_Lsp-expressing U87MG cells following exposure to all tested prodrugs. While the compounds exhibited toxicity to control cells at 100 μM, pronounced differences between control and CDA_Lsp-expressing cells were evident at prodrug concentrations of 5 μM and 10 μM,

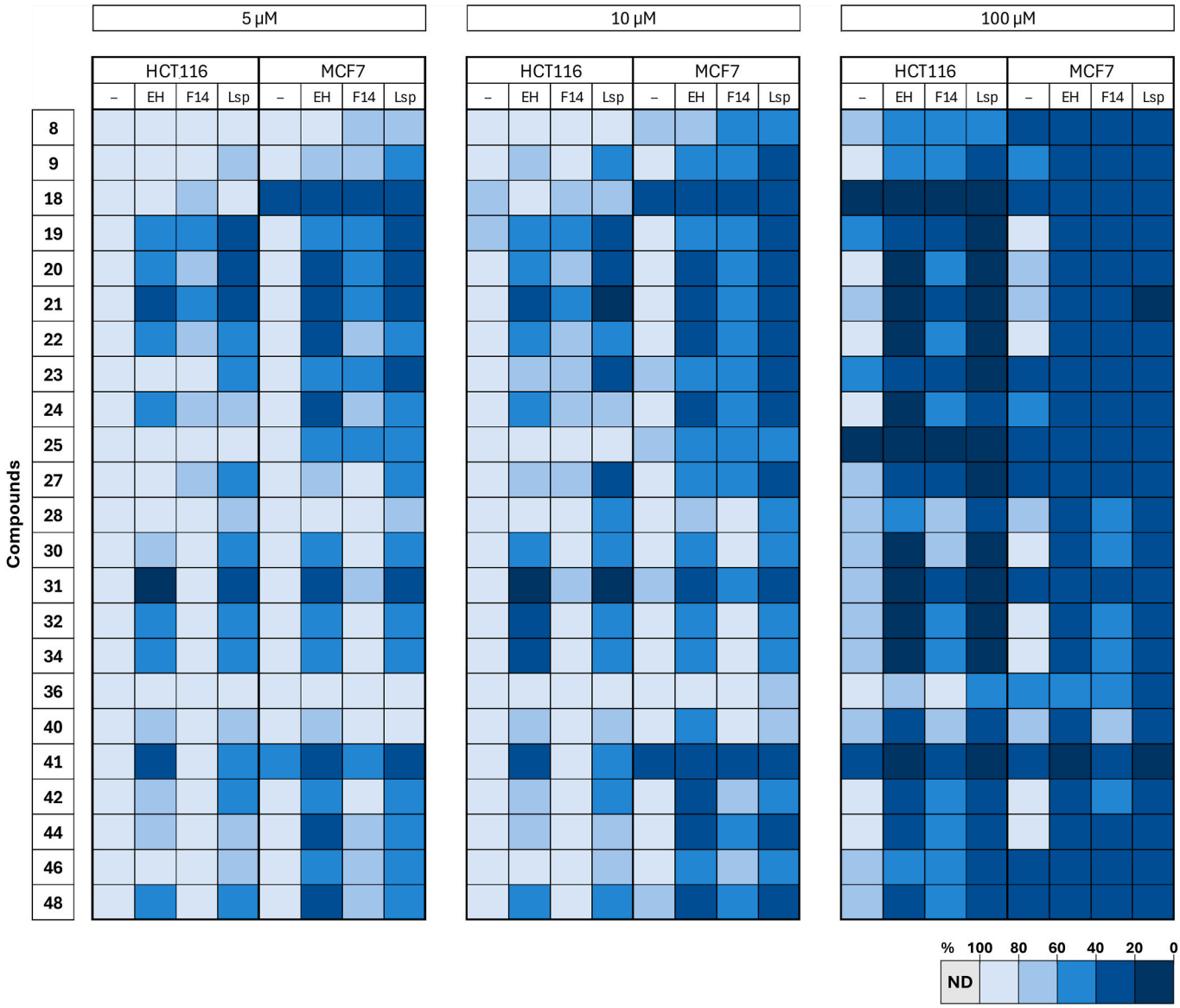

Fig. 7. Graphical representation of viability changes in HCT116 and MCF7 cell lines expressing human codon-optimized CDA_EH, CDA_F14, and CDA_Lsp following exposure to $S^4/N^4/O^4$-substituted 5-fluoropyrimidines. The cell lines were transduced with vectors encoding human-optimized CDA variants: pBABE-CDA_EH (designated as EH), pBABE-CDA_F14 (designated as F14), pBABE-CDA_Lsp (designated as Lsp), or the control vector pBABE-Puro (designated as symbol "–"). Cells were exposed to 5 μM, 10 μM, and 100 μM concentrations of the selected compounds for 48 h. ND – not determined.

thereby obviating the necessity for higher doses. These results confirm the efficacy of the CDA_Lsp-**19**/**21**/**30** enzyme-prodrug systems in reducing the viability of U87MG cancer cells and highlight the system's versatility across various cancer cell lines.

3. Discussion

In this study, we explored the ability of CDAs to activate prodrugs based on modified 5-fluoropyrimidine nucleosides. Three CDAs were selected for this investigation: CDA_EH and CDA_F14, which were identified in previous research through the analysis of metagenomic libraries, and CDA_Lsp, which was detected in the intestinal microbiota [31]. Due to its ability to catalyze the conversion of a broad spectrum of substrates, CDA_EH, CDA_F14, and CDA_Lsp were considered as promising candidates for prodrug activation studies. Notably, these enzymes catalyze the conversion of $S^4/N^4/O^4$-substituted pyrimidine nucleosides to uridine derivatives. We demonstrated that the substrate specificity of these CDAs can be significantly extended to include 5-fluoropyrimidine nucleosides with different modifications at the $S^4/N^4/O^4$ positions. This enzymatic activity offers potential applications in therapies that rely on forming toxic 5-FU or its nucleoside derivatives [32]. Several enzyme-prodrug therapies have been developed utilizing human CDA. For instance, the prodrug capecitabine is converted into 5-FU via a three-enzyme cascade, which includes human CDA [29]. Another example is the enzyme-prodrug system involving amidohydrolases and acylated 5-fluorocytidines, developed in our previous study, which produces 5-fluorocytidine [25]. This compound is then converted to the toxic 5-fluorouridine within cells, a process also reliant on human CDA. While these systems have demonstrated promising results, it is well known that the activity of human CDA can vary among individuals, reducing the general applicability of these therapies [26,33]. Additionally, the substrate specificity of human CDA is restricted, limiting the range of prodrugs that can be utilized [34]. In contrast, the CDAs examined in this study can directly convert modified 5-fluorocytidines into 5-fluorouridines, bypassing the need for additional enzymes, such as esterases or human CDA, in the prodrug activation process.

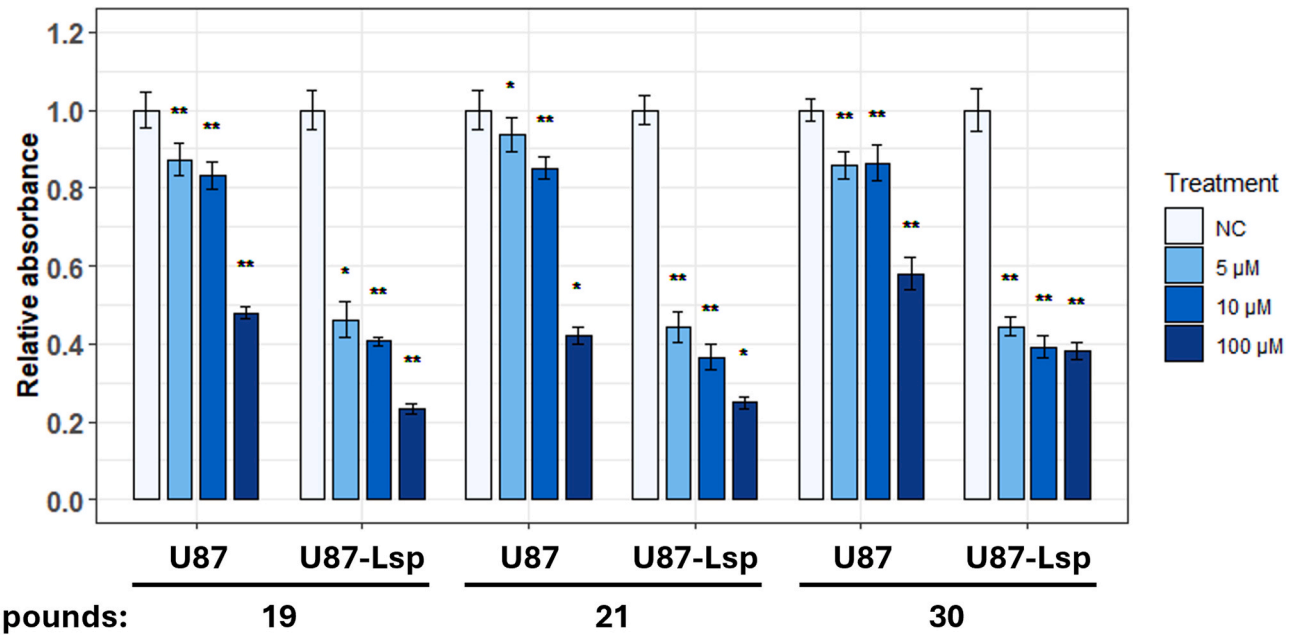

Fig. 8. MTT assay of U87MG cell line expressing CDA_Lsp following treatment of N^4/O^4-substituted 5-fluoropyrimidines. U87MG cell line expressing CDA_Lsp (designated as U87-Lsp) or control cell line (designated as U87) were exposed to three different concentrations (5 μM, 10 μM, and 100 μM) of compounds **19**, **21**, and **30** for 72 h. Statistical significance is indicated by *p*-values, where the symbol * designates $p < 0.05$, whereas the symbol ** designates $p < 0.01$ with respect to untreated cells (negative control (NC)). Each data point represents the mean of eight technical replicates (n = 8).

A range of modified 5-fluoropyrimidine nucleosides were evaluated as potential prodrugs, including N^4-acyl-5-fluorocytidines (**4**–**7**), 4-alkylthio-5-fluorouridines (**8**–**17**), N^4-alkyl-5-fluorocytidines (**18**–**24**), 4-alkoxy- and 4-aryloxy-5-fluorouridines (**25**–**41**), and 4-alkoxy-5-fluoro-2'-deoxyuridines (**42**–**49**). The broad selection of substrates was driven by the hypothesis that some might be activated by the investigated CDAs. Our results demonstrate that all analyzed nucleoside analogs, except for their acetylated forms, were converted to 5-fluorouridine or 5-fluoro-2′-deoxyuridine by CDA_EH, CDA_F14, and CDA_Lsp *in vitro*, with the exceptions of CDA_EH, which exhibited minimal activity toward 5-fluoro-N^4-methylcytidine (**18**), and CDA_F14 which showed no activity toward 5-fluoro-4-octylthiouridine (**17**). These findings suggest the potential for further expansion of the compound library, allowing for additional modifications at $S^4/N^4/O^4$ positions and variations between ribonucleosides and deoxyribonucleosides. Prior studies have examined collections of pyrimidine analogs with various modifications, assessing their potential for anti-cancer activity [35–37]. In contrast, our study provides a platform for screening modified nucleoside-based prodrugs using enzymes known to activate them. This approach establishes a systematic framework for evaluating new modified pyrimidine nucleosides as potential prodrug candidates.

We further demonstrated that the investigated compounds can be activated in cancer cell lines expressing bacterial CDA_EH, CDA_F14, and CDA_Lsp. Activation of N^4-acyl-5-fluorocytidines was successfully observed in the CDA_Lsp-expressing HCT116 cell line. In contrast, no significant differences between control and CDA_Lsp-expressing MCF7 cells were detected. These results align with the data from our previous study in which N^4-acyl-5-fluorocytidines were activated in HCT116, but not in MCF7 cell lines expressing bacterial amidohydrolases, suggesting cell type-specific response to N^4-acyl-5-fluorocytidines [25]. Furthermore, issues related to the chemical stability of N^4-acyl-5--fluorocytidines were noted during the experiments. Since prodrug strategies rely on the chemical stability of compounds [38], it was essential to continue research to identify compounds with more favorable prodrug properties. In this context, 4-alkylthio-5-fluorouridines exhibited greater chemical stability than N^4-acyl-5-fluorocytidines, though cell-specific responses were still observed. While no significant effects on MCF7 cell viability were noted, 4-alkylthio-5-fluorouridines significantly reduced the viability of bacterial CDA-expressing HCT116 cells, but only at the highest concentrations tested. This observation raises concerns for future studies, as anticancer agents are typically utilized at lower concentrations within the therapeutic window to avoid off-target toxicity [39]. Among the compounds tested, N^4-alkyl-5-fluorocytidines and 4-alkoxy-5-fluorouridines demonstrated the most significant potential as prodrugs. These compounds exhibited non-toxic effects on control cells even at higher concentrations and effectively reduced the viability of CDA-expressing cells at lower concentrations. However, each compound must be evaluated individually when analyzing the viability of bacterial CDA-expressing cells.

We established that the prodrugs were activated with varying efficiencies across different bacterial CDA-expressing cell lines. This variability can be attributed to the hypothesis that the synthesis of bacterial enzymes in eukaryotic cells is hindered by differences in codon usage and tRNA abundance between organisms [40]. The expression of recombinant bacterial enzymes in mammalian cells can be enhanced through codon optimization, which resolves the expression limitations associated with codon usage and maximizes protein expression [41,42]. Consequently, human codon-optimized variants of CDA_EH, CDA_F14, and CDA_Lsp were generated and integrated into the genomes of HCT116 and MCF7 cancer cell lines. The results indicated that codon optimization not only preserved the activity of the enzymes but also improved the prodrug conversion efficiency. However, differences in cell viability among the CDA_EH, CDA_F14, and CDA_Lsp-expressing cell lines after prodrug treatment remained, indicating that CDAs from different bacterial sources exhibit distinct substrate preferences. Nevertheless, the platform established in this study provides an efficient method for selecting the most suitable enzyme for activating specific prodrugs while also allowing for the integration of additional CDAs into the assays as necessary.

Potential activation of 23 modified 5-fluoropyrimidine nucleosides in HCT116 and MCF7 cancer cell lines expressing human-optimized CDA variants was investigated. All prodrugs tested demonstrated greater efficacy in cell lines expressing human-optimized CDAs than in those expressing bacterial CDAs. The previously observed tendency,

wherein N^4-alkyl-5-fluorocytidines and 4-alkoxy-5-fluorouridines exhibit greater potential as prodrugs than 4-alkylthio-5-fluorouridines, was also evident in these experimental conditions. This outcome can be attributed to two possible factors. First, CDA_EH, CDA_F14, and CDA_Lsp activate 5-fluoropyrimidines with different modifications at varying efficiencies [31], leading to differences in the formation of toxic metabolites within the cells. Second, nucleoside analogs are transported across the cell membrane with varying efficiencies [43], which may limit the entry of specific prodrugs, thus restricting their conversion to toxic metabolites. The analysis of acetylated and deacetylated variants of modified 5-fluoropyrimidines revealed notable differences in efficacy and toxicity to control cells. Acetylated 5-fluoropyrimidines at the 2', 3', and 5' positions were better tolerated at higher concentrations than their deacetylated analogs. This increased tolerance may be attributed to the stability of the compounds, as the presence of additional acetyl groups limits spontaneous transformation into toxic metabolites. The conversion of acetylated prodrugs to 5-fluorouridine or 5-fluoro-2′-deoxyuridine in cells expressing CDAs requires the involvement of intracellular esterases [44], enhancing the precision of the activation mechanism. When comparing free nucleosides **31** and **41** with their acetylated counterparts **30** and **40**, exposure to low concentrations of deacetylated analogs resulted in a more significant decrease in cell viability of CDA-expressing cells, likely due to the more rapid conversion to toxic metabolites. However, the relative non-toxicity of acetylated prodrugs to control cells makes them more promising candidates for further studies. Acetylated prodrugs are also preferred over their deacetylated counterparts because acetylation often enhances the bioavailability and transport of nucleosides across cell membranes, increasing their therapeutic potential [45]. Additionally, we found decreased cell viability in CDA-expressing cells upon exposure to 4-alkoxy-5-fluoro-2′-deoxyuridines tested. Given the distinct mechanisms of toxicity associated with 5-fluorouridine and 5-fluoro-2′-deoxyuridine [46], our findings suggest a possibility to expand the range of prodrugs tested by synthesizing both modified ribonucleoside and deoxyribonucleoside variants. This approach offers a significant advantage in addressing cellular resistance to anticancer agents, as once resistance to a specific ribonucleoside analog is observed, the platform facilitates the rapid selection and testing of its deoxyribonucleoside analog, or vice versa.

Finally, we evaluated the versatility of potential enzyme-prodrug combinations in other systems. Several compounds that demonstrated the most effective decrease in viability of CDA-expressing HCT116 and MCF7 cell lines were subsequently tested in the CDA_Lsp-expressing U87MG human glioblastoma cell line. Glioblastoma, known for its aggressive nature and resistance to many conventional chemotherapeutic agents, presents a significant challenge in cancer treatment [47]. The successful application of the enzyme-prodrug systems investigated in this study within glioblastoma cells would offer new opportunities for difficult-to-treat cancer research. The results indicated that exposure of N^4-propyl-5-fluorocytidine (**19**), N^4-pentyl-5-fluorocytidine (**21**), and acetylated 4-butoxy-5-fluorouridine (**30**) to CDA_Lsp-expressing U87MG cells effectively reduced cell viability. This finding highlights the efficacy of the CDA_Lsp-**19**/**21**/**30** combinations across different cell line origins. Ultimately, this platform could be translated into clinical settings through targeted gene delivery strategies, enabling tumor-specific expression of selected CDAs to locally activate 5-fluoropyrimidine prodrugs and reduce systemic toxicity. However, further studies are required to validate the broader applicability of these strategies, including testing in additional cancer cell lines and more complex experimental models.

In conclusion, this study introduced a platform designed to efficiently screen modified 5-fluoropyrimidine nucleosides as potential prodrugs, utilizing CDAs of bacterial origin. We identified several enzyme-prodrug combinations that effectively reduced cancer cell viability. Additionally, we demonstrated the potential of N^4-alkyl-5-fluorocytidines and 4-alkoxy-5-fluorouridines as prodrugs. Finally, our platform supports a wide range of 5-fluoropyrimidine analogs and diverse activating enzymes, making it a flexible and effective tool for rapidly identifying and evaluating new targets for further studies.

4. Experimental section

4.1. Chemicals

5-Fluorouridine (**1**) was purchased from Thermo Fisher Scientific (Lithuania), while 5-fluoro-2′-deoxyuridine (**3**) was obtained from Apollo Scientific (UK). Compounds **4**, **5**, **6**, **7** [25], as well as **2**, **8**, **9**, **25**, **30**, **31**, **40**, **41** [31], were synthesized as described previously. The synthesis of 3′,5′-di-*O*-acetyl-5-fluoro-2′-deoxyuridine and 2′,3′,5′-tri--*O*-acetyl-5-fluoro-4-thiouridine was performed according to previously reported procedure [31]. Detailed synthesis of the remaining compounds is provided below in this section. ^{1}H NMR, ^{13}C NMR, and ^{19}F NMR spectra (SM, Fig. S1–S63 in Section S1) were recorded in $CDCl_3$ or DMSO-d_6 on Bruker Ascend 400 spectrometer, at 400 MHz for ^{1}H NMR, 101 MHz for ^{13}C NMR and 376 MHz for ^{19}F NMR. Chemical shifts are reported in parts per million (ppm) relative to solvent resonance signal. Coupling constants are reported in Hz. All compounds are >95 % pure by HPLC (SM, Table S2 and Fig. S64–S85 in Section S2).

High-resolution mass spectra were acquired using Agilent 6224 A TOF LC-MS system equipped with Agilent 1260 Infinity HPLC and positive electrospray ionization (ESI+). Separations were carried out on Dr. Maisch ReproSil-Pur Basic-C18 100 × 2.1 mm, 1.9 μm column. The mobile phase A was 0.1 % formic acid in deionised water (v/v), while mobile phase B was 0.1 % formic acid in acetonitrile (v/v). Column was maintained at 50 °C, with a flow rate of 0.4 mL/min. A 10 min linear gradient from 5 % B to 100 % B was used followed by 2 min isocratic hold at 100 % B. The following parameters were used for MS analysis: gas temperature: 300 °C; gas flow: 8 mL/min; nebulizer: 30 psig; capillary: 3000 V; fragmentor: 125 V.

General synthesis scheme

General procedure for the synthesis of 2′,3′,5′-tri-O-acetyl-5-fluoro-4-alkylthiouridines (10, 12, 14, 16), 2′,3′,5′-tri-O-acetyl-5-fluoro-4-alkoxyuridines (26, 28, 32, 34, 36), 2′,3′,5′-tri-O-acetyl-5-fluoro-4-phenoxyuridine (38), and 3′,5′-di-O-acetyl-5-fluoro-4-alkoxy-2′-deoxyuridines (42, 44, 46, 48)

$POCl_3$ (2.2 eq) was added dropwise to a suspension of 1,2,4-triazole (10 eq.) in MeCN (1 M) at −5 °C, followed by the dropwise addition of triethylamine (10 eq.). Reaction was stirred in the ice bath for 1 h, then solution of 2′,3′,5′-tri-*O*-acetyl-5-fluorouridine (**2**) or 3′,5′-di-*O*-acetyl-5-fluoro-2′-deoxyuridine (1 eq.) in MeCN (0.1 M) was added and reaction was left to stir and slowly warm up to room temperature overnight. After TLC analysis (DCM:MeOH:acetone 30:1:1) confirmed full consumption of starting material, reaction mixture was diluted with water and product was extracted with DCM (× 3). Combined organic phases were washed with brine (× 1), dried over Na_2SO_4, filtered, and concentrated. Crude mixture was redissolved in MeCN (0.3 M) and corresponding alcohol, thiol or phenol (1.2 eq.) was added to it at room temperature, followed by the addition of DIPEA (1.2 eq.). After the intermediate triazolyl adduct was fully consumed (TLC, DCM:MeOH:acetone 50:1:1), reaction mix was diluted with water and product was extracted with DCM (× 4). Combined organic phases were washed once with brine, then dried over Na_2SO_4, filtered and concentrated. Products from 2′,3′,5′-tri-*O*-acetyl-5-fluorouridine were purified with column chromatography using mixture of DCM:MeOH:acetone as eluent (200:1:1 to 50:1:1). Products from 3′,5′-di-*O*-acetyl-5-fluoro-2′-deoxyuridine were purified with column chromatography using mixture of DCM:MeOH: acetone as eluent (400:1:1 to 100:1:1).

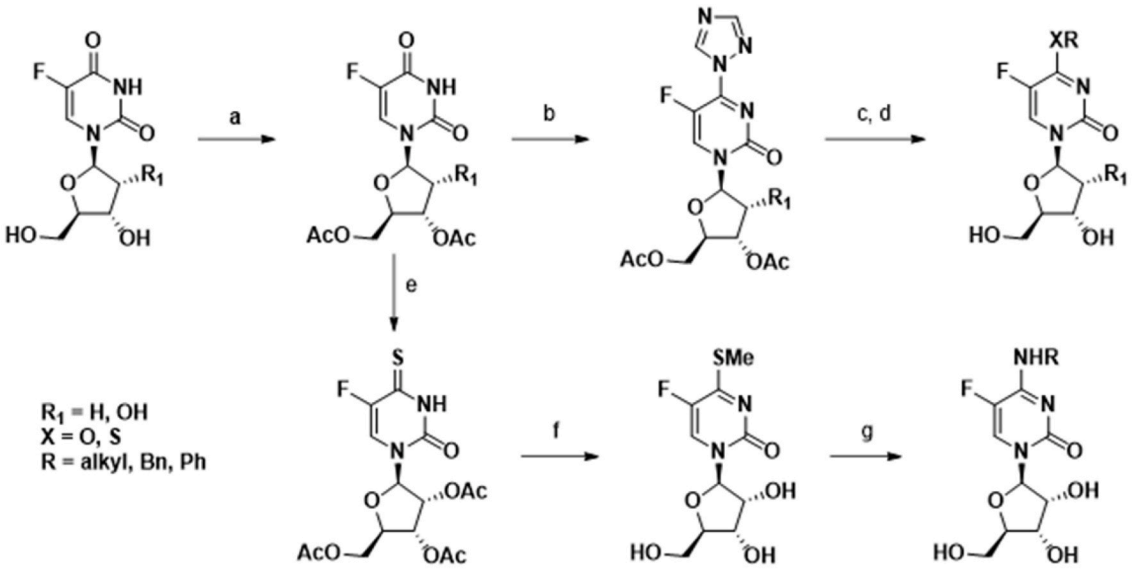

2′,3′,5′-tri-O-acetyl-5-fluoro-4-butylthiouridine (10)

The compound **10** was isolated as a colorless glassy oil (95 mg) 53 % yield over 2 steps from 0.4 mmol of 2′,3′,5′-tri-*O*-acetyl-5-fluorouridine (**2**), and 1-buthanethiol. R_f = 0.25 [DCM:MeOH:acetone (100:1:1)]; ^{1}H NMR (400 MHz, $CDCl_3$) δ 7.69 (d, *J* = 5.1 Hz, 1H), 6.08 (d, *J* = 3.9 Hz, 1H), 5.41–5.34 (m, 1H), 5.28 (t, *J* = 5.6 Hz, 1H), 4.45–4.35 (m, 3H), 3.24 (t, *J* = 7.3 Hz, 2H), 2.16 (s, 3H), 2.12 (s, 3H), 2.09 (s, 3H), 1.69 (p, *J* = 7.4 Hz, 2H), 1.46 (h, *J* = 7.3 Hz, 2H), 0.94 (t, *J* = 7.3 Hz, 3H); ^{13}C NMR (101 MHz, $CDCl_3$) δ 171.2 (d, *J* = 17.3 Hz), 170.1, 169.7, 169.5, 151.9, 143.8 (d, *J* = 243.7 Hz), 123.2 (d, *J* = 34.6 Hz), 88.8, 79.9, 73.9, 69.5, 62.6, 30.6, 29.1 (d, *J* = 1.7 Hz), 22.1, 20.8, 20.6, 20.6, 13.7; ^{19}F NMR (376 MHz, $CDCl_3$) δ −155.4 (d, *J* = 5.0 Hz); HRMS (ESI) calcd for $C_{19}H_{25}O_8N_2SF$: 460.13156; found 460.13052.

2′,3′,5′-tri-O-acetyl-5-fluoro-4-isobutylthiouridine (12)

The compound **12** was isolated as a colorless glassy oil (45 mg) 25 % yield over 2 steps from 0.4 mmol of 2′,3′,5′-tri-*O*-acetyl-5-fluorouridine (**2**), and 2-methylpropane-1-thiol. R_f = 0.3 [DCM:MeOH:acetone (100:1:1)]; ^{1}H NMR (400 MHz, $CDCl_3$) δ 7.69 (d, *J* = 5.1 Hz, 1H), 6.07 (d, *J* = 3.9 Hz, 1H), 5.40–5.33 (m, 1H), 5.31–5.24 (m, 1H), 4.44–4.35 (m, 3H), 3.16 (d, *J* = 6.8 Hz, 2H), 2.15 (s, 3H), 2.11 (s, 3H), 2.08 (s, 3H), 1.99 (hept, *J* = 6.7 Hz, 1H), 1.04 (d, *J* = 6.7 Hz, 6H); ^{13}C NMR (101 MHz, $CDCl_3$) δ 171.2 (d, *J* = 17.1 Hz), 170.1, 169.6, 169.5, 151.8, 143.9 (d, *J* = 243.7 Hz), 123.2 (d, *J* = 34.6 Hz), 88.8, 79.9, 73.9, 69.5, 62.6, 37.5 (d, *J* = 1.5 Hz), 28.0, 22.0, 22.0, 20.8, 20.6; ^{19}F NMR (376 MHz, $CDCl_3$) δ −155.3 (d, *J* = 4.9 Hz); HRMS (ESI) calcd for $C_{19}H_{25}O_8N_2SF$: 460.13156; found 460.13041.

2′,3′,5′-tri-O-acetyl-5-fluoro-4-hexylthiouridine (14)

The compound **14** was isolated as a colorless glassy oil (110 mg) 54 % yield over 2 steps from 0.4 mmol of 2′,3′,5′-tri-*O*-acetyl-5-fluorouridine (**2**), and 1-hexanethiol. R_f = 0.6 [DCM:MeOH:acetone (50:1:1)]; ^{1}H NMR (400 MHz, $CDCl_3$) δ 7.69 (dd, *J* = 5.2, 1.0 Hz, 1H), 6.07 (d, *J* = 4.0 Hz, 1H), 5.37 (dd, *J* = 5.3, 4.0 Hz, 1H), 5.28 (t, *J* = 5.6 Hz, 1H), 4.44–4.35 (m, 3H), 3.23 (t, *J* = 7.3 Hz, 2H), 2.15 (s, 3H), 2.11 (s, 3H), 2.08 (s, 3H), 1.70 (p, *J* = 7.6 Hz, 2H), 1.42 (p, *J* = 7.1 Hz, 2H), 1.36–1.23 (m, 4H), 0.87 (t, *J* = 6.5 Hz, 3H); ^{13}C NMR (101 MHz, $CDCl_3$) δ 171.2 (d, *J* = 17.3 Hz), 170.1, 169.6, 169.5, 151.9, 143.8 (d, *J* = 243.6 Hz), 123.2 (d, *J* = 34.7 Hz), 88.8, 79.9, 73.9, 69.5, 62.6, 31.4, 29.4 (d, *J* = 1.7 Hz), 28.6, 28.4, 22.6, 20.8, 20.6, 20.6, 14.1; ^{19}F NMR (376 MHz, $CDCl_3$) δ −155.3 (d, *J* = 5.2 Hz); HRMS (ESI) calcd for $C_{21}H_{29}O_8N_2SF$: 488.16286; found 488.16189.

2′,3′,5′-tri-O-acetyl-5-fluoro-4-octylthiouridine (16)

The compound **16** was isolated as a colorless glassy oil (130 mg) 53 % yield over 2 steps from 0.4 mmol of 2′,3′,5′-tri-*O*-acetyl-5-fluorouridine (**2**), and 1-octanethiol. R_f = 0.6 [DCM:MeOH:acetone (50:1:1)]; ^{1}H NMR (400 MHz, $CDCl_3$) δ 7.69 (d, *J* = 5.1 Hz, 1H), 6.07 (d, *J* = 3.5 Hz, 1H), 5.37 (dd, *J* = 5.4, 3.9 Hz, 1H), 5.28 (t, *J* = 5.7 Hz, 1H), 4.45–4.35 (m, 3H), 3.22 (t, *J* = 7.2 Hz, 2H), 2.15 (s, 3H), 2.11 (s, 3H), 2.08 (s, 3H), 1.69 (p, *J* = 7.5 Hz, 2H), 1.41 (p, *J* = 7.6 Hz, 2H), 1.35–1.20 (m, 8H), 0.90–0.82 (m, 3H); ^{13}C NMR (101 MHz, $CDCl_3$) δ 171.2 (d, *J* = 17.3 Hz), 170.1, 169.6, 169.5, 151.9, 143.8 (d, *J* = 243.6 Hz), 123.2 (d, *J* = 34.7 Hz), 88.8, 79.9, 73.9, 69.5, 62.6, 31.9, 29.4 (d, *J* = 1.6 Hz), 29.2, 29.2, 28.9, 28.5, 22.7, 20.8, 20.6, 20.6, 14.2; ^{19}F NMR (376 MHz, $CDCl_3$) δ −155.3 (d, *J* = 4.3 Hz); HRMS (ESI) calcd for $C_{23}H_{33}O_8N_2SF$: 516.19416; found 516.19322.

2′,3′,5′-tri-O-acetyl-5-fluoro-4-ethoxyuridine (26)

The compound **26** was isolated as a colorless glassy oil (78 mg) 72 % yield over 2 steps from 0.26 mmol of 2′,3′,5′-tri-*O*-acetyl-5-fluorouridine (**2**), and ethanol. R_f = 0.35 [DCM:MeOH:acetone (50:1:1)]; ^{1}H NMR (400 MHz, $CDCl_3$) δ 7.79 (d, *J* = 5.8 Hz, 1H), 6.14 (dd, *J* = 4.3, 1.5 Hz, 1H), 5.34 (dd, *J* = 5.4, 4.3 Hz, 1H), 5.27 (t, *J* = 5.3 Hz, 1H), 4.52 (qd, *J* = 7.1, 1.4 Hz, 2H), 4.42–4.30 (m, 3H), 2.15 (s, 3H), 2.10 (s, 3H), 2.08 (s, 3H), 1.41 (t, *J* = 7.1 Hz, 3H); ^{13}C NMR (101 MHz, $CDCl_3$) δ 170.1, 169.7, 169.6, 162.8 (d, *J* = 12.9 Hz), 153.4, 137.2 (d, *J* = 248.9 Hz), 126.3 (d, *J* = 32.2 Hz), 88.3, 79.9, 73.7, 69.7, 64.7, 62.7, 20.8, 20.6, 14.2; ^{19}F NMR (376 MHz, $CDCl_3$) δ −167.3 (d, *J* = 5.5 Hz); HRMS (ESI) calcd for $C_{17}H_{21}O_9N_2F$: 416.12311; found 416.12184.

2′,3′,5′-tri-O-acetyl-5-fluoro-4-propoxyuridine (28)

The compound **28** was isolated as a colorless glassy oil (343 mg) 80 % yield over 2 steps from 1 mmol of 2′,3′,5′-tri-*O*-acetyl-5-fluorouridine (**2**), and 1-propanol. R_f = 0.45 [DCM:MeOH:acetone (50:1:1)]; ^{1}H NMR (400 MHz, $CDCl_3$) δ 7.8 (d, *J* = 5.7 Hz, 1H), 6.2 (d, *J* = 4.3 Hz, 1H), 5.3 (t, *J* = 4.9 Hz, 1H), 5.3 (t, *J* = 5.3 Hz, 1H), 4.4–4.3 (m, 5H), 2.2 (s, 3H), 2.1 (s, 3H), 2.1 (s, 3H), 1.8 (h, *J* = 7.1 Hz, 2H), 1.0 (t, *J* = 7.4 Hz, 3H);

^{13}C NMR (101 MHz, $CDCl_3$) δ 170.2, 169.7, 169.6, 162.9 (d, J = 13.0 Hz), 153.5, 137.2 (d, J = 248.8 Hz), 126.3 (d, J = 32.0 Hz), 88.2, 79.8, 73.7, 70.2, 69.7, 62.7, 21.9, 20.9, 20.6, 10.3; ^{19}F NMR (376 MHz, $CDCl_3$) δ −167.2 (d, J = 6.1 Hz); HRMS (ESI) calcd for $C_{18}H_{23}O_9N_2F$: 430.13876; found 430.13786.

2′,3′,5′-tri-O-acetyl-5-fluoro-4-pentoxyuridine (32)

The compound **32** was isolated as a colorless glassy oil (444 mg) 71 % yield over 2 steps from 1.37 mmol of 2′,3′,5′-tri-*O*-acetyl-5-fluorouridine (**2**), and 1-pentanol. R_f = 0.45 [DCM:MeOH:acetone (50:1:1)]; ^{1}H NMR (400 MHz, $CDCl_3$) δ 7.80 (d, J = 5.8 Hz, 1H), 6.15 (dd, J = 4.4, 1.5 Hz, 1H), 5.34 (t, J = 4.9 Hz, 1H), 5.32–5.24 (m, 1H), 4.44 (td, J = 6.8, 2.0 Hz, 2H), 4.42–4.35 (m, 3H), 2.16 (s, 3H), 2.11 (s, 3H), 2.09 (s, 3H), 1.79 (p, J = 7.1 Hz, 2H), 1.45–1.28 (m, 4H), 0.91 (t, J = 6.9 Hz, 3H); ^{13}C NMR (101 MHz, $CDCl_3$) δ 170.2, 169.7, 169.6, 162.9 (d, J = 12.9 Hz), 153.5, 137.2 (d, J = 248.9 Hz), 126.2 (d, J = 32.3 Hz), 88.2, 79.8, 73.7, 69.6, 68.9, 62.7, 28.1, 27.9, 20.9, 20.6, 14.1; ^{19}F NMR (376 MHz, $CDCl_3$) δ −167.2 (d, J = 5.6 Hz); HRMS (ESI) calcd for $C_{20}H_{27}O_9N_2F$: 458.17006; found 458.16921.

2′,3′,5′-tri-O-acetyl-5-fluoro-4-hexoxyuridine (34)

The compound **34** was isolated as a colorless glassy oil (407 mg) 63 % yield over 2 steps from 1.37 mmol of 2′,3′,5′-tri-*O*-acetyl-5-fluorouridine (**2**), and 1-hexanol. R_f = 0.4 [DCM:MeOH:acetone (50:1:1)]; ^{1}H NMR (400 MHz, $CDCl_3$) δ 7.80 (d, J = 5.7 Hz, 1H), 6.15 (dd, J = 4.4, 1.5 Hz, 1H), 5.34 (t, J = 4.9 Hz, 1H), 5.32–5.24 (m, 1H), 4.44 (td, J = 6.8, 2.0 Hz, 2H), 4.42–4.34 (m, 3H), 2.16 (s, 3H), 2.11 (s, 3H), 2.09 (s, 3H), 1.78 (p, J = 6.9 Hz, 2H), 1.46–1.34 (m, 2H), 1.35–1.28 (m, 4H), 0.88 (t, J = 6.8 Hz, 3H); ^{13}C NMR (101 MHz, $CDCl_3$) δ 170.2, 169.7, 169.6, 162.9 (d, J = 13.0 Hz), 153.5, 137.2 (d, J = 248.8 Hz), 126.2 (d, J = 32.2 Hz), 88.2, 79.8, 73.7, 69.6, 68.9, 62.7, 31.5, 28.4, 25.5, 22.6, 20.9, 20.6, 14.1; ^{19}F NMR (376 MHz, $CDCl_3$) δ −167.2 (d, J = 5.7 Hz); HRMS (ESI) calcd for $C_{21}H_{29}O_9N_2F$: 472.18571; found 472.18466.

2′,3′,5′-tri-O-acetyl-5-fluoro-4-propargyloxyuridine (36)

The compound **36** was isolated as a colorless glassy oil (513 mg) 80 % yield over 2 steps from 1.5 mmol of 2′,3′,5′-tri-*O*-acetyl-5-fluorouridine (**2**), and propargyl alcohol. R_f = 0.45 [DCM:MeOH:acetone (50:1:1)]; ^{1}H NMR (400 MHz, $CDCl_3$) δ 7.89 (d, J = 5.6 Hz, 1H), 6.12 (dd, J = 4.2, 1.5 Hz, 1H), 5.39–5.32 (m, 1H), 5.32–5.24 (m, 1H), 4.45–4.31 (m, 3H), 2.59 (t, J = 2.4 Hz, 1H), 2.16 (s, 3H), 2.11 (s, 3H), 2.09 (s, 3H); ^{13}C NMR (101 MHz, $CDCl_3$) δ 170.1, 169.7, 169.6, 161.6 (d, J = 13.2 Hz), 152.9, 136.7 (d, J = 249.3 Hz), 127.3 (d, J = 31.7 Hz), 88.4, 79.9, 76.7, 76.5, 73.8, 69.5, 62.6, 55.7, 20.9, 20.6; ^{19}F NMR (376 MHz, $CDCl_3$) δ −167.2 (d, J = 5.6 Hz); HRMS (ESI) calcd for $C_{18}H_{19}O_9N_2F$: 426.10746; found 426.10645.

2′,3′,5′-tri-O-acetyl-5-fluoro-4-phenoxyuridine (38)

The compound **38** was isolated as a colorless glassy oil (58 mg) 48 % yield over 2 steps from 0.26 mmol of 2′,3′,5′-tri-*O*-acetyl-5-fluorouridine (**2**), and phenol. R_f = 0.45 [DCM:MeOH:acetone (50:1:1)]; ^{1}H NMR (400 MHz, $CDCl_3$) δ 7.98 (d, J = 5.6 Hz, 1H), 7.40 (t, J = 7.9 Hz, 2H), 7.30–7.21 (m, 1H), 7.22–7.16 (m, 2H), 6.11 (dd, J = 4.2, 1.5 Hz, 1H), 5.36 (dd, J = 5.4, 4.1 Hz, 1H), 5.29 (t, J = 5.4 Hz, 1H), 4.45–4.33 (m, 3H), 2.19 (s, 3H), 2.10 (s, 3H), 2.09 (s, 3H); ^{13}C NMR (101 MHz, $CDCl_3$) δ 170.1, 169.7, 169.5, 162.3 (d, J = 12.8 Hz), 152.8, 151.0, 136.8 (d, J = 249.6 Hz), 129.8, 127.9 (d, J = 31.9 Hz), 126.6, 121.6, 88.6, 80.0, 73.8, 69.6, 62.6, 20.9, 20.6; ^{19}F NMR (376 MHz, $CDCl_3$) δ −166.6 (d, J = 5.9 Hz); HRMS (ESI) calcd for $C_{21}H_{21}O_9N_2F$: 464.12311; found 464.12190.

3′,5′-di-O-acetyl-5-fluoro-4-butoxy-2′-deoxyuridine (42)

The compound **42** was isolated as a colorless glassy oil (521 mg) 90 % yield over 2 steps from 1.5 mmol of 3′,5′-di-*O*-acetyl-5-fluoro-2′-deoxyuridine, and 1-butanol. R_f = 0.75 [DCM:MeOH:acetone (50:1:1)]; ^{1}H NMR (400 MHz, $CDCl_3$) δ 7.81 (d, J = 5.9 Hz, 1H), 6.26 (ddd, J = 7.5, 5.6, 1.7 Hz, 1H), 5.18 (dt, J = 6.6, 2.6 Hz, 1H), 4.44 (t, J = 6.7 Hz, 2H), 4.39–4.27 (m, 3H), 2.70 (ddd, J = 14.3, 5.7, 2.6 Hz, 1H), 2.14–2.02 (m, 7H), 1.82–1.70 (m, 2H), 1.50–1.36 (m, 2H), 0.94 (t, J = 7.4 Hz, 3H); ^{13}C NMR (101 MHz, $CDCl_3$) δ 170.5, 170.3, 162.7 (d, J = 12.8 Hz), 153.4, 137.0 (d, J = 247.8 Hz), 126.2 (d, J = 32.0 Hz), 86.8, 82.7, 73.9, 68.4, 63.7, 38.8, 30.5, 21.0, 20.9, 19.1, 13.8; ^{19}F NMR (376 MHz, $CDCl_3$) δ −167.9 (d, J = 5.4 Hz); HRMS (ESI) calcd for $C_{17}H_{23}O_7N_2F$: 386.14893; found 386.14815.

3′,5′-di-O-acetyl-5-fluoro-4-hexyloxy-2′-deoxyuridine (44)

The compound **44** was isolated as slightly yellow glassy oil (603 mg) 97 % yield over 2 steps from 1.5 mmol of 3′,5′-di-*O*-acetyl-5-fluoro-2′-deoxyuridine and 1-hexanol. R_f = 0.7 [DCM:MeOH:acetone (50:1:1)]; ^{1}H NMR (400 MHz, $CDCl_3$) δ 7.81 (d, J = 5.9 Hz, 1H), 6.26 (ddd, J = 7.5, 5.6, 1.7 Hz, 1H), 5.19 (dt, J = 6.1, 2.7 Hz, 1H), 4.44 (t, J = 6.8 Hz, 2H), 4.40–4.33 (m, 2H), 4.33–4.26 (m, 1H), 2.71 (ddd, J = 14.3, 5.7, 2.6 Hz, 1H), 2.14–2.03 (m, 7H), 1.78 (p, J = 6.9 Hz, 2H), 1.50–1.35 (m, 2H), 1.37–1.26 (m, 4H), 0.93–0.83 (m, 3H); ^{13}C NMR (101 MHz, $CDCl_3$) δ 170.5, 170.3, 162.7 (d, J = 12.7 Hz), 153.4, 137.0 (d, J = 247.9 Hz), 126.2 (d, J = 32.0 Hz), 86.8, 82.8, 73.9, 68.8, 63.7, 38.8, 31.5, 28.4, 25.5, 22.6, 21.0, 20.9, 14.1; ^{19}F NMR (376 MHz, $CDCl_3$) δ −167.91 (d, J = 5.2 Hz); HRMS (ESI) calcd for $C_{19}H_{27}O_7N_2F$: 414.18023; found 414.17935.

3′,5′-di-O-acetyl-5-fluoro-4-propargyloxy-2′-deoxyuridine (46)

The compound **46** was isolated as a colorless glassy oil (432 mg) 78 % yield over 2 steps from 1.5 mmol of 3′,5′-di-*O*-acetyl-5-fluoro-2′-deoxyuridine, and propargyl alcohol. R_f = 0.7 [DCM:MeOH:acetone (50:1:1)]; ^{1}H NMR (400 MHz, $CDCl_3$) δ 7.90 (d, J = 5.6 Hz, 1H), 6.28–6.19 (m, 1H), 5.19 (dt, J = 6.1, 2.7 Hz, 1H), 5.10–5.00 (m, 2H), 4.38 (dd, J = 12.8, 4.2 Hz, 1H), 4.35–4.29 (m, 2H), 2.73 (ddd, J = 14.3, 5.6, 2.6 Hz, 1H), 2.57 (t, J = 2.4 Hz, 1H), 2.15–2.04 (m, 7H); ^{13}C NMR (101 MHz, $CDCl_3$) δ 170.5, 170.2, 161.3 (d, J = 13.1 Hz), 152.8, 136.5 (d, J = 248.3 Hz), 127.2 (d, J = 31.6 Hz), 87.0, 82.9, 76.6, 76.6, 73.8, 63.7, 55.6, 38.8, 21.0, 20.9; ^{19}F NMR (376 MHz, $CDCl_3$) δ −167.8 (d, J = 5.4 Hz); HRMS (ESI) calcd for $C_{16}H_{17}O_7N_2F$: 368.10198; found 368.10127.

3′,5′-di-O-acetyl-5-fluoro-4-benzyloxy-2′-deoxyuridine (48)

The compound **48** was isolated as a colorless glassy oil (540 mg) 86 % yield over 2 steps from 1.5 mmol of 3′,5′-di-*O*-acetyl-5-fluoro-2′-deoxyuridine, and benzyl alcohol. R_f = 0.7 [DCM:MeOH:acetone (50:1:1)]; ^{1}H NMR (400 MHz, $CDCl_3$) δ 7.86 (d, J = 5.7 Hz, 1H), 7.51–7.42 (m, 2H), 7.42–7.33 (m, 3H), 6.27 (ddd, J = 7.4, 5.6, 1.6 Hz, 1H), 5.55–5.43 (m, 2H), 5.19 (dt, J = 6.6, 2.7 Hz, 1H), 4.42–4.27 (m, 3H), 2.73 (ddd, J = 14.3, 5.7, 2.6 Hz, 1H), 2.18–2.03 (m, 7H); ^{13}C NMR (101 MHz, $CDCl_3$) δ 170.5, 170.2, 162.3 (d, J = 12.9 Hz), 153.2, 136.8 (d, J = 248.0 Hz), 134.7, 128.8, 128.8, 128.7, 126.7 (d, J = 31.9 Hz), 86.9, 82.8, 73.9, 69.8, 63.7, 38.8, 21.0, 20.8; ^{19}F NMR (376 MHz, $CDCl_3$) δ −167.64 (dd, J = 5.9, 1.9 Hz); HRMS (ESI) calcd for $C_{20}H_{21}O_7N_2F$: 420.13328; found 420.13239.

General procedure for the deacetylation of 2′,3′,5′-tri-*O*-acetyl-5-fluoro-4-alkoxyuridines (27, 29, 33, 35).

Acetylated derivatives **26**, **28**, **32**, and **34** were deacetylated to yield compounds **27**, **29**, **33**, and **35**, respectively, as follows: the corresponding acylated compounds (prepared as 100 mM stock solutions in methanol) were added in portions to reaction mixtures containing 50 mM potassium phosphate buffer (pH 7.5) and 0.5 mg/mL of esterase Gru1 (GenBank accession no. MH423265) [48]. The final concentration of each substrate in the reaction mixture was 5–10 mM. Reactions were incubated at 37 °C for up to 4 h with shaking. The deacetylation process was monitored by TLC using chloroform:methanol (5:1) as the mobile phase. Reaction products were purified using a FlashPure Select C18 column (30 μm spherical, 20 g) with a water/methanol gradient (95:5 → 0:100). Fractions containing the desired compounds were pooled and concentrated using a rotary evaporator. Compounds were

synthesized on 5–20 mmol scale and were used in further experiments without additional characterization.

General procedure for synthesis of 5-fluoro-N^4-alkylcytidines (18–24)

Na_2CO_3 (3.2 eq, 0.32 mmol) and RNH_2 (1 eq, 0.1 mmol) were added to a 0.6 M solution of 5-fluoro-S^4-methylthiouridine (3 eq, 0.3 mmol) in water at room temperature. After 48 h, the reaction mixture was concentrated under reduced pressure. Products were purified by flash chromatography (FlashPure Select C18 20 g column, H_2O:MeOH 95:5 to 0:100).

5-Fluoro-N^4-methylcytidine (18)

The compound **18** was isolated as white amorphous solid (20 mg, 24 %). R_f = 0.3 [$CHCl_3$:MeOH (5:1)]; ^{1}H NMR (400 MHz, DMSO-d_6) δ 8.18 (d, *J* = 7.6 Hz, 1H), 8.00 (s, 1H), 5.71 (dd, *J* = 3.8, 1.9 Hz, 1H), 5.25 (s, 3H), 3.93 (dd, *J* = 15.4, 4.9 Hz, 2H), 3.82 (dt, *J* = 5.6, 2.8 Hz), 3.69 (dd, *J* = 12.1, 2.9 Hz, 1H), 3.56 (dd, *J* = 12.1, 2.8 Hz), 2.80 (s, 3H); ^{13}C NMR (101 MHz, DMSO-d_6) δ 155.4 (d, *J* = 13.3 Hz), 153.5, 136.5 (d, *J* = 240.3 Hz), 124.3 (d, *J* = 32.2 Hz), 89.2, 83.9, 74.2, 68.9, 60.1, 26.9; ^{19}F NMR (376 MHz, DMSO-d_6) δ - 169.48 (d, *J* = 6.5 Hz); HRMS (ESI) calcd for $C_{10}H_{14}O_5N_3F$: 275.09175; found 275.09100.

5-Fluoro-N^4-propylcytidine (19)

The compound **19** was isolated as white amorphous solid (34 mg, 37 %). R_f = 0.4 [$CHCl_3$:MeOH (5:1)]; ^{1}H NMR (400 MHz, DMSO-d_6) δ 8.18 (d, *J* = 7.5 Hz, 1H), 8.05 (s, 1H), 5.71 (dd, *J* = 3.8, 1.9 Hz, 1H), 5.24 (s, 3H), 3.93 (dq, *J* = 8.8, 4.8 Hz, 2H), 3.82 (dt, *J* = 5.5, 2.8 Hz, 1H), 3.69 (dd, *J* = 12.1, 3.0 Hz, 1H), 3.56 (dd, *J* = 12.1, 2.8 Hz, 1H), 3.25 (t, *J* = 7.3 Hz, 2H), 1.53 (h, *J* = 7.4 Hz, 2H), 0.84 (t, *J* = 7.4 Hz, 3H); ^{13}C NMR (101 MHz, DMSO-d_6) δ 155.0 (d, *J* = 13.2 Hz), 153.6, 136.3 (d, *J* = 240.6 Hz), 124.5 (d, *J* = 32.5 Hz), 89.2, 83.9, 74.2, 69.0, 60.1, 41.4, 21.7, 11.3; ^{19}F NMR (376 MHz, DMSO-d_6) δ −168.92 (d, *J* = 6.6 Hz); HRMS (ESI) calcd for $C_{12}H_{18}O_5N_3F$: 303.12305; found 303.12227.

5-Fluoro-N^4-butylcytidine (20)

The compound **20** was isolated as white amorphous solid (20 mg, 21 %). R_f = 0.45 [$CHCl_3$:MeOH (5:1)]; ^{1}H NMR (400 MHz, DMSO-d_6) δ 8.17 (d, *J* = 7.5 Hz, 1H), 8.03 (s, 1H), 5.71 (dd, *J* = 3.8, 1.9 Hz, 1H), 5.21 (s, 3H), 3.93 (dq, *J* = 8.7, 4.8 Hz, 2H), 3.82 (dt, *J* = 5.5, 2.8 Hz, 1H), 3.69 (dd, *J* = 12.1, 2.9 Hz, 1H), 3.56 (dd, *J* = 12.2, 2.8 Hz, 1H), 3.29 (t, *J* = 7.3 Hz, 2H), 1.50 (p, *J* = 7.3 Hz, 2H), 1.28 (hept, *J* = 7.5 Hz, 2H), 0.88 (t, *J* = 7.3 Hz, 3H); ^{13}C NMR (101 MHz, DMSO-d_6) δ 155.4 (d, *J* = 13.2 Hz), 154.0, 136.8 (d, *J* = 241.0 Hz), 124.9 (d, *J* = 32.4 Hz), 89.6, 84.4, 74.6, 69.4, 60.6, 39.8, 31.0, 20.1, 14.2; ^{19}F NMR (376 MHz, DMSO-d_6) δ −168.91 (d, *J* = 7.3 Hz); HRMS (ESI) calcd for $C_{13}H_{20}O_5N_3F$: 317.13870; found 317.13789.

5-Fluoro-N^4-pentylcytidine (21)

The compound **21** was isolated as white amorphous solid (46 mg, 46 %). R_f = 0.5 [$CHCl_3$:MeOH (5:1)]; ^{1}H NMR (400 MHz, DMSO-d_6) δ 8.18 (d, *J* = 7.5 Hz, 1H), 8.04 (s, 1H), 5.71 (dd, *J* = 3.8, 1.9 Hz, 1H), 5.24 (s, 3H), 3.94 (dq, *J* = 8.7, 4.8 Hz, 2H), 3.82 (dt, *J* = 5.5, 2.8 Hz, 1H), 3.69 (dd, *J* = 12.1, 2.9 Hz, 1H), 3.57 (dd, *J* = 12.1, 2.8 Hz, 1H), 3.29 (t, *J* = 7.3 Hz, 2H), 1.52 (p, *J* = 7.3 Hz, 2H), 1.38–1.20 (m, 4H), 0.87 (t, *J* = 6.8 Hz, 3H); ^{13}C NMR (101 MHz, DMSO-d_6) δ 154.9 (d, *J* = 13.0 Hz), 154.0, 136.8 (d, *J* = 240.9 Hz), 124.9 (d, *J* = 32.6 Hz), 89.6, 84.4, 74.6, 69.5, 60.6, 40.1, 29.0, 28.6, 22.4, 14.4; ^{19}F NMR (376 MHz, DMSO-d_6) δ −168.93 (d, *J* = 6.5 Hz); HRMS (ESI) calcd for $C_{14}H_{23}O_5N_3F$: 331.15435; found 331.15338.

5-Fluoro-N^4-hexylcytidine (22)

The compound **22** was isolated as white amorphous solid (44 mg, 39 %). R_f = 0.5 [$CHCl_3$:MeOH (5:1)]; ^{1}H NMR (400 MHz, DMSO-d_6) δ 8.17 (d, *J* = 7.6 Hz, 1H), 8.04 (s, 1H), 5.70 (dd, *J* = 3.8, 1.9 Hz, 1H), 5.15–5.31 (m, 3H), 3.95 (t, *J* = 5.1 Hz, 1H), 3.91 (t, *J* = 4.4 Hz, 1H), 3.82 (dt, *J* = 5.5, 2.8 Hz, 1H), 3.69 (dd, *J* = 12.1, 2.9 Hz, 1H), 3.56 (dd, *J* = 12.2, 2.8 Hz, 1H), 3.28 (t, *J* = 7.3 Hz, 2H), 1.50 (p, *J* = 6.8 Hz, 2H), 1.25 (s, 6H), 0.82–0.88 (m, 3H); ^{13}C NMR (101 MHz, DMSO-d_6) δ 154.8 (d, *J* = 13.2 Hz), 153.7, 136.4 (d, *J* = 240.7 Hz), 124.6 (d, *J* = 32.4 Hz), 89.2, 84.0, 74.3, 69.0, 60.2, 39.8, 31.1, 28.5, 26.2, 22.2, 14.0; ^{19}F NMR (376 MHz, DMSO-d_6) δ −168.83 (d, *J* = 7.5 Hz); HRMS (ESI) calcd for $C_{15}H_{24}O_5N_3F$: 345.17000; found 345.16925.

5-Fluoro-N^4-propargylcytidine (23)

The compound **23** was isolated as white amorphous solid (74 mg, 90 %). R_f = 0.35 [$CHCl_3$:MeOH (5:1)])]; ^{1}H NMR (400 MHz, DMSO-d_6) δ 8.47 (t, *J* = 5.8 Hz, 1H), 8.28 (d, *J* = 7.4 Hz, 1H), 5.70 (dd, *J* = 3.5, 1.9 Hz, 1H), 5.44 (s, 1H), 5.27 (s, 1H), 5.05 (s, 1H), 4.09 (dt, *J* = 5.8, 2.8 Hz, 2H), 3.94–3.99 (m, 1H), 3.92 (t, *J* = 4.2 Hz, 1H), 3.83 (dt, *J* = 5.6, 2.8 Hz, 1H), 3.70 (dd, *J* = 12.2, 2.9 Hz, 1H), 3.57 (dd, 12.2, 2.7 Hz, 1H), 2.07 (s, 1H); ^{13}C NMR (101 MHz, DMSO-d_6) δ 154.7 (d, *J* = 13.6 Hz), 153.3, 136.2 (d, *J* = 240.5 Hz), 125.4 (d, *J* = 32.3 Hz), 89.4, 84.0, 80.7, 74.4, 68.9, 60.0, 29.0; ^{19}F NMR (376 MHz, DMSO-d_6) δ −169.13 (d, *J* = 7.4 Hz); HRMS (ESI) calcd for $C_{12}H_{14}O_5N_3F$: 299.09175; found 299.09108.

5-Fluoro-N^4-benzylcytidine (24)

The compound **24** was isolated as white amorphous solid (68 mg, 65 %).

R_f = 0.5 [$CHCl_3$:MeOH (5:1)]; ^{1}H NMR (400 MHz, DMSO-d_6) δ 8.57 (s, 1H), 8.24 (d, *J* = 7.5 Hz, 1H), 7.35–7.31 (m, 2H), 7.31–7.28 (m, 2H), 7.27–7.21 (m, 1H), 5.71 (dd, *J* = 3.7, 1.9 Hz, 1H), 5.28 (s, 3H), 4.55 (s, 2H), 3.99–3.95 (m, 1H), 3.93 (dd, *J* = 4.9, 3.7 Hz, 1H), 3.83 (dt, *J* = 5.4, 2.8 Hz, 1H), 3.70 (dd, *J* = 12.1, 2.9 Hz, 1H), 3.57 (dd, *J* = 12.2, 2.8 Hz, 1H); ^{13}C NMR (101 MHz, DMSO-d_6) δ 155.0 (d, *J* = 13.3 Hz), 153.5, 138.8, 136.3 (d, *J* = 240.7 Hz), 128.3 (2C), 127.2 (2C), 126.9, 125.0 (d, *J* = 32.5 Hz), 89.3, 84.0, 74.2, 69.0, 60.1, 42.7; ^{19}F NMR (376 MHz, DMSO-d_6) δ −169.48 (s); HRMS (ESI) calcd for $C_{16}H_{18}O_5N_3F$: 351.12305; found 351.12228.

4.2. Enzymatic activity measurements

The procedures for cloning, expression, and purification of recombinant CDA_EH, CDA_F14, and CDA_Lsp enzymes, as well as the enzymatic activity with particular compounds, were described previously [31]. For all other compounds, enzymatic reactions were carried out in a reaction buffer consisting of 10 mM Tris-HCl (pH 7.5). Substrates (**10**–**24**, **26**–**29**, **32**–**39**, **42**–**49**) were prepared at a final concentration of 200 μM. The reactions included the enzymes CDA_EH, CDA_F14, and CDA_Lsp, each at a final concentration of 2 μM. When de-acetylation was required, Gru1 esterase [48] was added to the reaction mixture to achieve a final concentration of 10 μM. All reactions were incubated at 37 °C for 1 h. To terminate the reactions, the mixtures were combined with an equal volume of acetonitrile, centrifuged at 30000×*g* for 10 min, and 0.5–1 μL of the supernatant was analyzed using liquid chromatography-tandem mass spectrometry (LC-MS). The analysis was conducted on a Nexera X2 UHPLC system coupled with an LCMS-8050 mass spectrometer (Shimadzu, Japan), equipped with an electrospray ionization (ESI) source operating in both negative and positive ionization modes. Chromatographic separation was performed using a 3 × 150 mm YMC-Triart C18 column with a particle size of 3 μm (YMC, Japan) at 40 °C. The mobile phase consisted of 0.1 % formic acid (solvent A) and acetonitrile (solvent B), delivered in gradient elution mode at a flow rate of 0.45 mL/min. The following gradient program was used: 0–1 min, 5 % solvent B; 1–5 min, 95 % solvent B; 5–7 min, 95 % solvent B; 7–8 min, 5 % solvent B; 8–12 min, 5 % solvent B. Mass scans were recorded from *m/z* 50 to *m/z* 750, with an interface temperature of 300 °C and a desolvation line temperature of 250 °C. Nitrogen (N_2) was used as the nebulizing gas at 3 l/min and drying gas at 10 l/min, while dry air was used as the heating gas at 10 l/min. Data analysis was performed using LabSolutions LCMS software (Shimadzu).

4.3. Plasmid constructs

The DNA fragment, encoding His-tagged deaminase CDA_EH, CDA_F14, or CDA_Lsp flanked by the unique restriction sites *Bam*HI and *Eco*105I, was cloned into vector pBABE-Puro (Cell Biolabs, Inc., USA) using *Bam*HI and *Eco*105I restriction sites. Genes encoding CDA_EH, CDA_F14, and CDA_Lsp (the sequences of *cda_eh, cda_f14*, and *cda_lsp* genes were described in a previous publication [31]) were PCR-amplified using 2 × Phusion Polymerase Master Mix (Thermo Fisher Scientific, Lithuania) and the following pairs of primers: EH_*Bam*HI_FW (5′-TGACGGATCCATGAAGGAAACACTTTG-3′) and Cdd_*Eco*105I_RV (5′-TGACTACGTATTAGCCGTGGTGGTGATG-3′) for *cda_eh*, F14_*Bam*HI_FW (5′- TGACGGATCCATGAACAAGGAAGATTT-3′) and Cdd_*Eco*105I_RV for *cda_f14*, Lsp_*Bam*HI_FW (5′-TGACGGATCCATGCGTGACAAACTGA-3′) and Cdd_*Eco*105I_RV for *cda_lsp*. The PCR products were digested with *Bam*HI and *Eco*105I (Thermo Fisher Scientific, Lithuania) and ligated to pBABE-Puro using T4 DNA Ligase (Thermo Fisher Scientific, Lithuania) according to the manufacturer's instructions. Constructs were sequence-verified by Azenta (Germany). The DNA fragments, encoding C-terminally FLAG-tagged human codon-optimized version of deaminase sequences, were synthesized and subcloned into pMA-RQ by GeneArt service (Thermo Fisher Scientific, Lithuania). The resulting sequences were subcloned into the pBABE-Puro vector via flanking restriction sites *Bam*HI and *Eco*105I. The expression vector pTO/Lsp was generated by subcloning the BamHI – NotI DNA fragment from pMA-RQ/Lsp into vector pcDNA4/TO (Invitrogen) using *Bam*HI and *Not*I restriction sites.

4.4. Cell culturing

All procedures were performed under aseptic conditions, adhering to biological safety requirements. The human embryonal kidney-derived cell line 293FT was obtained from Invitrogen, USA (catalog No. R70007). The human colon cancer cell line HCT116 (ATCC CCL-247, Thermo Fisher Scientific, catalog No. 50-238-3906) and the human breast cancer cell line MCF7 (ATCC HTB-22, Thermo Fisher Scientific, catalog No. 50-238-4386) were a gift from Dr. Daiva Baltriukienė (Life Sciences Center, Vilnius University, Vilnius, Lithuania). The human glioblastoma cell line U87MG was obtained from the European Collection of Cell Cultures (ECACC, catalog No. 89081402). 293FT cells were cultured in Dulbecco's Modified Eagle's Medium (DMEM; Gibco, USA) supplemented with 10 % fetal bovine serum (FBS, Gibco, USA), 0.1 mM MEM Non-Essential Amino Acids (NEAA, Gibco, USA), 6 mM l-glutamine (Gibco, USA), 1 mM MEM sodium pyruvate (Gibco, USA), 100 U/mL penicillin, 0.1 mg/mL streptomycin (Gibco, USA), and 0.5 mg/mL geneticin (Gibco, USA). HCT116, MCF7, and U87MG cells were routinely propagated in DMEM supplemented with 10 % FBS, 100 U/mL penicillin, and 0.1 mg/mL streptomycin. Cells were incubated at 37 °C in a humidified atmosphere of 95 % air and 5 % CO_2. For passaging, cells were detached using trypsin/EDTA (Gibco, USA) at 37 °C.

4.5. Generation of cell lines

HCT116 and MCF7 cell lines expressing CDA_EH, CDA_F14, and CDA_Lsp deaminases were generated following the protocol described previously [25]. U87-CDA_Lsp cell line, which stably expressed CDA_Lsp, was generated by transfecting U87MG cells with linearized (ScaI restriction) vector pTO/CDA_Lsp and performing multiple rounds of selection of cells that were resistant to zeocin (500 μg/mL; Gibco, USA). At the final selection stage, cells were propagated and examined for the expression of CDA_Lsp by Western blot analysis, as described below in this section.

4.6. Expression analysis of mRNA

Total RNA was extracted from transduced HCT116 and MCF7 cell lines using TRIzol Reagent (Thermo Fisher Scientific, Vilnius, Lithuania), and the cDNA synthesis was performed with Maxima H Minus First Strand cDNA Synthesis Kit with dsDNase (Thermo Fisher Scientific, Vilnius, Lithuania), according to the manufacturer's instructions. The mRNA expressions of *cda_eh*, *cda_f14*, and *cda_lsp* were analyzed by Real-Time Quantitative PCR (RT-qPCR) using Luminaris Color HiGreen High ROX kit (Thermo Fisher Scientific, Lithuania). The primers for the bacterial genes included: EH_qPCR_FW (5′-ATGCCTACTGCCCGTATTCC-3′), EH_qPCR_RV (5′-CTTAAAGATGGCCGTCCGCT-3′) for *cda_eh* (137 bp amplicon size), F14_qPCR_FW (5′-GCCTATGCCCCGTATTCCAA-3′), F14_qPCR_RV (5′-TGCAGCGAAAATGGCACTTC-3′) for *cda_f14* (138 bp amplicon size), and Lsp_qPCR_FW (5′-GGTGCGGACGGTGTTATCTA-3′), Lsp_qPCR_RV (5′-TTACCGTTGCAAACAACCGC-3′) for *cda_lsp* (146 bp amplicon size). The primers for human-optimized genes were used as follows: EH_Hopt_qPCR_FW (5′-GCTGCAACATCGAGAACACC-3′), EH_Hopt_qPCR_RV (5′-AAGGGGCACCATCAGCTTC-3′) for *cda_eh* (138 bp amplicon size), F14_Hopt_qPCR_FW (5′-CCGATGATATCGAGGCCCTG-3′), F14_Hopt_qPCR_RV (5′-CAGTGTCTCTTTGCCGTTGC-3′) for *cda_f14* (137 bp amplicon size), and Lsp_Hopt_qPCR_FW (5′-CCTGTGGGAGCTGCTGTTAT-3′), Lsp_Hopt_qPCR_RV (5′-GTATAGGTCTGGCAGCCGTG-3′) for *cda_lsp* (140 bp amplicon size). In each set of RT-qPCR analyses, two negative controls were used: nuclease-free water and cells expressing "empty" control vector pBABE-Puro. Amplification parameters for all the *cda_eh*, *cda_f14*, and *cda_lsp* were those offered by the manufacturer.

4.7. Whole-cell extract preparation and Western blot analysis

Whole-cell extracts of HCT116 and MCF7 cell lines expressing CDA_EH, CDA_F14 or CDA_Lsp deaminases were prepared by resuspending the cell pellet in RIPA lysis buffer (50 mM TRIS-HCl; 1.5 M NaCl, pH 7.6; 1 % Triton X-100; 5 mM sodium dodecyl sulfate; 25 mM sodium deoxycholate; 1 % phenylmethylsulfonyl fluoride, 0.2 % aprotinin, 0.2 % sodium orthovanadate). The extracts were cleared by centrifugation for 15 min at 12000×*g* at 4 °C. Subsequently, total extract proteins were fractionated by 14 % SDS-PAGE and transferred onto the 0.2 μm polyvinylidene fluoride (PVDF) membrane (PVDF Western Blotting Membranes 0.2 μm, Merck). After the blocking for 1 h in 2 % bovine serum albumin dissolved in Tris-buffered saline (TBS), the immobilized proteins were incubated overnight at 4 °C with the primary mouse monoclonal antibody against 6 × His Tag (Thermo Scientific™; catalog No. MA1-21315, dilution 1:1000) or the primary rabbit monoclonal antibody against FLAG epitope Tag (DYKDDDDK Tag, Thermo Scientific™; catalog No. 701629, dilution 1:250) in blocking solution. After extensive washing in TBS-T buffer (TBS supplemented with 0.05 % Tween-20), membranes were incubated with the horseradish peroxidase- (HRP-) conjugated anti-mouse (Carl Roth, Germany; catalog No. 4759, dilution 1:10000) or anti-rabbit (Elabscience, USA; catalog No. E-AB-1003, dilution 1:10000) secondary antibody for 1 h at 22 °C. Immunocomplexes were visualized using an enhanced chemiluminescence substrate (Pierce ECL Western Blotting Substrate, Thermo Scientific™) and documented by the Uvitec Alliance imaging system (Uvitec Cambridge, United Kingdom).

Whole-cell extracts of U87MG cells (negative control) and U87-CDA_Lsp cells expressing FLAG-tagged protein CDA_Lsp were routinely prepared by resuspending the cell pellet in modified RIPA lysis buffer (50 mM Tris-HCl, pH 7.5, 150 mM NaCl, 1 % Igepal CA-630, 0.5 % sodium deoxycholate, 0.1 % SDS) supplemented with a protease inhibitor cocktail (Sigma-Aldrich). Subsequently, the extracts were cleared by centrifugation for 30 min at 13000×*g* at 4 °C. 60 μg of the total extract protein was fractionated by 15 % SDS-PAGE and transferred onto the 0.1 μm nitrocellulose membrane (Amersham Protran Sandwich 0.1 μm, Merck). After the blocking overnight in 5 % nonfat milk dissolved in phosphate-buffered saline (PBS), the immobilized proteins were incubated for 3 h at 25 °C with the primary rabbit monoclonal antibody against FLAG epitope tag, diluted as 1:500 in blocking solution. After

extensive washing in PBS-T buffer (PBS supplemented with 0.5 % Tween-20), membranes were incubated with the horseradish peroxidase- (HRP-) conjugated anti-rabbit secondary antibody (Invitrogen, catalog No. 65–6120, dilution 1:2000) for 40 min at 25 °C. Immunocomplexes were visualized using a chromogenic substrate 3,3',5,5'-tetramethylbenzidine (TMB, Sigma-Aldrich) and documented by an image scanner.

4.8. MTT assays

The viability of cells treated with different compounds in 96 well plates was examined by a 3-(4,5-dimethyl-2-thiazolyl)-2,5-diphenyl-2-H-tetrazolium bromide (MTT) assay. Solutions of all tested compounds were prepared fresh for each experiment in DMSO diluted in the complete culture medium and added to HCT116, MCF7, or U87MG cells to a final concentration of 1–100 μM. The concentration of DMSO in the assay never exceeded 0.02 % and had no influence on cell growth. The MTT assay for HCT116 and MCF7 cells was performed according to the previously described protocol [25]. The MTT assay for U87 cells was performed as described next: U87MG (control) and U87-Lsp cells were seeded onto 96-well plates (2500 cells per well). The next day, cell culture media was replaced with media containing different concentrations of chemicals or DMSO as vehicle control. After 72 h of incubation, cells were washed with PBS, and 80 μL of the MTT/cell medium mixture (0.5 μg/mL of the final MTT reagent concentration) was added to each well. After 3 h of incubation at 37 °C, this mixture was replaced by 100 μL DMSO. The intensity (absorbance) of the colored formazan product was measured at 550 and 620 nm by Multiskan GO Microplate Spectrophotometer (Thermo Fisher Scientific). Prior to performing the statistical analysis, the obtained data was processed in two steps: first, the 620 nm measurements (background) were subtracted from individual 550 nm measurements; next, the data obtained from cell sample groups treated with different test reagents was normalized against the sample group treated with DMSO.

4.9. Statistical analysis

All grouped MTT analysis data was presented as mean with a 95 % confidence interval. Comparisons between groups were made by the one-tailed Welch's *t*-test for independent samples. The Shapiro-Wilk test was performed to evaluate deviation from normality. The significance level was chosen at $\alpha = 0.05$ for all criteria used. Data were plotted, and statistical analysis was performed using RStudio version March 1, 1073.

CRediT authorship contribution statement

Viktorija Preitakaitė: Writing – review & editing, Writing – original draft, Visualization, Methodology, Investigation, Conceptualization. **Arūnas Kazlauskas:** Writing – review & editing, Methodology, Investigation. **Agota Aučynaitė:** Writing – review & editing, Methodology, Investigation. **Kamilė Butkutė:** Writing – review & editing, Methodology, Investigation. **Ringailė Lapinskaitė:** Writing – review & editing, Methodology, Investigation. **Nina Urbelienė:** Writing – review & editing, Methodology, Investigation. **Audrius Laurynėnas:** Writing – review & editing, Funding acquisition. **Rolandas Meškys:** Writing – review & editing, Supervision, Resources, Conceptualization.

Declaration of competing interest

V.P., R.M. and N.U. declare potential financial interests in the future development and commercialization of cytidine deaminases. Vilnius University has filed an EPO patent application (EP23168045). All other authors declare no competing financial or non-financial interests.

Acknowledgment

This project has received funding from the Research Council of Lithuania (LMTLT), agreement No S-MIP-24-114. The funders had no role in study design, data collection and analysis, decision to publish, or preparation of the manuscript.

Appendix B. Supplementary data

Supplementary data to this article can be found online at https://doi.org/10.1016/j.ejmech.2025.117860.

Abbreviations Used

5-FC, 5-fluorocytosine; 5-FIC, 5-fluoroisocytosine; 5-FU, 5-fluorouracil; CD, cytosine deaminase; CDA, cytidine deaminase; EPT, Enzyme-prodrug therapy; GDEPT, gene-directed enzyme-prodrug therapy; ICD, isocytosine deaminase; SM, supplementary material.

Data availability

Data will be made available on request.

References

[1] J. Rautio, H. Kumpulainen, T. Heimbach, R. Oliyai, D. Oh, T. Järvinen, et al., Prodrugs: design and clinical applications, Nat. Rev. Drug Discov. 7 (2008) 255–270, https://doi.org/10.1038/nrd2468.
[2] S. Zhao, N. Yu, H. Han, S. Guo, N. Murthy, Advances in acid-degradable and enzyme-cleavable linkers for drug delivery, Curr. Opin. Chem. Biol. 84 (2025) 102552, https://doi.org/10.1016/j.cbpa.2024.102552.
[3] R. Walther, J. Rautio, A.N. Zelikin, Prodrugs in medicinal chemistry and enzyme prodrug therapies, Adv. Drug Deliv. Rev. 118 (2017) 65–77, https://doi.org/10.1016/j.addr.2017.06.013.
[4] J.B. Zawilska, J. Wojcieszak, A.B. Olejniczak, Prodrugs: a challenge for the drug development, Pharmacol. Rep. 65 (2013) 1–14, https://doi.org/10.1016/S1734-1140(13)70959-9.
[5] B. Parshad, S. Arora, B. Singh, Y. Pan, J. Tang, Z. Hu, et al., Towards precision medicine using biochemically triggered cleavable conjugation, Commun. Chem. 8 (2025) 1–16, https://doi.org/10.1038/s42004-025-01491-5.
[6] N. Schellmann, P.M. Deckert, D. Bachran, H. Fuchs, C. Bachran, Targeted enzyme prodrug therapies, Mini Rev. Med. Chem. 10 (2010) 887–904, https://doi.org/10.2174/138955710792007196.
[7] J. Zhang, V. Kale, M. Chen, Gene-directed enzyme prodrug therapy, AAPS J. 17 (2015) 102–110, https://doi.org/10.1208/s12248-014-9675-7.
[8] Ly CY. Shin, A.P. Kunnath, Application of gene-directed enzyme prodrug therapy in cancer treatment, Int. J. Biomed. Res. Pract. 1 (2021), https://doi.org/10.33425/2769-6294.1004.
[9] D.A. Hamstra, K.C. Lee, J.M. Tychewicz, V.D. Schepkin, B.A. Moffat, M. Chen, et al., The use of 19F spectroscopy and diffusion-weighted MRI to evaluate differences in gene-dependent enzyme prodrug therapies, Mol. Ther. J. Am. Soc. Gene Ther. 10 (2004) 916–928, https://doi.org/10.1016/j.ymthe.2004.07.022.
[10] A.S.A. El-Sayed, N.Z. Mohamed, M.A. Yassin, M.M. Amer, R. El-Sharkawy, N. El-Sayed, et al., Microbial cytosine deaminase is a programmable anticancer prodrug mediating enzyme: antibody, and gene directed enzyme prodrug therapy, Heliyon 8 (2022) e10660, https://doi.org/10.1016/j.heliyon.2022.e10660.
[11] C.J. Springer, I. Niculescu-Duvaz, Gene-directed enzyme prodrug therapy (GDEPT): choice of prodrugs, Adv. Drug Deliv. Rev. 22 (1996) 351–364, https://doi.org/10.1016/S0169-409X(96)00449-8.
[12] K. Kurozumi, T. Tamiya, Y. Ono, S. Otsuka, H. Kambara, Y. Adachi, et al., Apoptosis induction with 5-fluorocytosine/cytosine deaminase gene therapy for human malignant glioma cells mediated by adenovirus, J. Neuro Oncol. 66 (2004) 117–127, https://doi.org/10.1023/b:neon.0000013494.98345.80.
[13] M. Berg, C. Li, S. Kaiser, NAIL-MS reveals tRNA and rRNA hypomodification as a consequence of 5-fluorouracil treatment, Nucleic Acids Res. 53 (2025) gkaf090, https://doi.org/10.1093/nar/gkaf090.
[14] S. Aberle, N. Schug, R. Mathlouthi, G. Seitz, J.-H. Küpper, K. Schröder, et al., Promoter selection for the cytosine deaminase suicide gene constructs in gastric cancer, Eur. J. Gastroenterol. Hepatol. 16 (2004) 63–67, https://doi.org/10.1097/00042737-200401000-00010.
[15] Y. Chen, J. Ye, Z. Zhu, W. Zhao, J. Zhou, C. Wu, et al., Comparing paclitaxel plus fluorouracil versus cisplatin plus fluorouracil in chemoradiotherapy for locally advanced esophageal squamous cell cancer: a randomized, multicenter, phase III clinical trial, J. Clin. Oncol. 37 (2019) 1695–1703, https://doi.org/10.1200/JCO.18.02122.
[16] L. Negroni, M. Samson, J.-M. Guigonis, B. Rossi, V. Pierrefite-Carle, C. Baudoin, Treatment of colon cancer cells using the cytosine deaminase/5-fluorocytosine suicide system induces apoptosis, modulation of the proteome, and Hsp90beta

phosphorylation, Mol. Cancer Therapeut. 6 (2007) 2747–2756, https://doi.org/10.1158/1535-7163.MCT-07-0040.
[17] T. Miyagi, K. Koshida, O. Hori, H. Konaka, H. Katoh, Y. Kitagawa, et al., Gene therapy for prostate cancer using the cytosine deaminase/uracil phosphoribosyltransferase suicide system, J. Gene Med. 5 (2003) 30–37, https://doi.org/10.1002/jgm.317.
[18] C. Yi, Y. Huang, Z. Guo, S. Wang, Antitumor effect of cytosine deaminase/5-fluorocytosine suicide gene therapy system mediated by Bifidobacterium infantis on melanoma, Acta Pharmacol. Sin. 26 (2005) 629–634, https://doi.org/10.1111/j.1745-7254.2005.00094.x.
[19] S.-Q. Lv, K.-B. Zhang, E.E. Zhang, F.-Y. Gao, C.-L. Yin, C.-J. Huang, et al., Antitumor efficiency of the cytosine deaminase/5-fluorocytosine suicide gene therapy system on malignant gliomas: an in vivo study, Med. Sci. Monit. Int. Med. J. Exp. Clin. Res. 15 (2009) BR13–BR20.
[20] S. Sheikh, D. Ernst, A. Keating, Prodrugs and prodrug-activated systems in gene therapy, Mol. Ther. 29 (2021) 1716–1728, https://doi.org/10.1016/j.ymthe.2021.04.006.
[21] M. Fuchita, A. Ardiani, L. Zhao, K. Serve, B.L. Stoddard, M.E. Black, Bacterial cytosine deaminase mutants created by molecular engineering demonstrate improved 5FC-Mediated cell killing in vitro and in vivo, Cancer Res. 69 (2009) 4791–4799, https://doi.org/10.1158/0008-5472.CAN-09-0615.
[22] L.-Y. Deng, J.-P. Wang, Z.-F. Gui, L.-Z. Shen, Antitumor activity of mutant bacterial cytosine deaminase gene for colon cancer, World J. Gastroenterol. 17 (2011) 2958–2964, https://doi.org/10.3748/wjg.v17.i24.2958.
[23] Z. Karjoo, X. Chen, A. Hatefi, Progress and problems with the use of suicide genes for targeted cancer therapy, Adv. Drug Deliv. Rev. 99 (2016) 113–128, https://doi.org/10.1016/j.addr.2015.05.009.
[24] A. Kazlauskas, A. Darinskas, R. Meškys, A. Tamašauskas, J. Urbonavičius, Isocytosine deaminase Vcz as a novel tool for the prodrug cancer therapy, BMC Cancer 19 (2019) 197, https://doi.org/10.1186/s12885-019-5409-7.
[25] V. Preitakaitė, P. Barasa, A. Aučynaitė, G. Plakys, M. Koplūnaitė, S. Zubavičiūtė, et al., Bacterial amidohydrolases and modified 5-fluorocytidine compounds: novel enzyme-prodrug pairs, PLoS One 18 (2023) e0294696, https://doi.org/10.1371/journal.pone.0294696.
[26] C. Serdjebi, G. Milano, J. Ciccolini, Role of cytidine deaminase in toxicity and efficacy of nucleosidic analogs, Expert Opin. Drug Metab. Toxicol. 11 (2015) 665–672, https://doi.org/10.1517/17425255.2015.985648.
[27] F. Di Costanzo, A. Sdrobolini, S. Gasperoni, Capecitabine, a new oral fluoropyrimidine for the treatment of colorectal cancer, Crit. Rev. Oncol. Hematol. 35 (2000) 101–108, https://doi.org/10.1016/S1040-8428(00)00059-7.
[28] B. Javdan, J.G. Lopez, P. Chankhamjon, Y.-C.J. Lee, R. Hull, Q. Wu, et al., Personalized mapping of drug metabolism by the human gut microbiome, Cell 181 (2020) 1661–1679.e22, https://doi.org/10.1016/j.cell.2020.05.001.
[29] S.W. Lam, H.J. Guchelaar, E. Boven, The role of pharmacogenetics in capecitabine efficacy and toxicity, Cancer Treat Rev. 50 (2016) 9–22, https://doi.org/10.1016/j.ctrv.2016.08.001.
[30] D. Micozzi, F.M. Carpi, S. Pucciarelli, V. Polzonetti, P. Polidori, S. Vilar, et al., Human cytidine deaminase: a biochemical characterization of its naturally occurring variants, Int. J. Biol. Macromol. 63 (2014) 64–74, https://doi.org/10.1016/j.ijbiomac.2013.10.029.
[31] N. Urbelienė, M. Tiškus, G. Tamulaitienė, R. Gasparavičiūtė, R. Lapinskaitė, V. Jauniškis, et al., Cytidine deaminases catalyze the conversion of N(S,O)4-substituted pyrimidine nucleosides, Sci. Adv. 9 (2023) eade4361, https://doi.org/10.1126/sciadv.ade4361.
[32] N. Zhang, Y. Yin, S.-J. Xu, W.-S. Chen, 5-Fluorouracil: Mechanisms of resistance and reversal strategies, Molecules 13 (2008) 1551–1569, https://doi.org/10.3390/molecules13081551.
[33] A. Frances, P. Cordelier, The emerging role of cytidine deaminase in human diseases: a new opportunity for therapy? Mol. Ther. J. Am. Soc. Gene Ther. 28 (2020) 357–366, https://doi.org/10.1016/j.ymthe.2019.11.026.
[34] T. Cacciamani, A. Vita, G. Cristalli, S. Vincenzetti, P. Natalini, S. Ruggieri, et al., Purification of human cytidine deaminase: molecular and enzymatic characterization and inhibition by synthetic pyrimidine analogs, Arch. Biochem. Biophys. 290 (1991) 285–292, https://doi.org/10.1016/0003-9861(91)90543-R.
[35] F. Xie, H. Zhao, L. Zhao, L. Lou, Y. Hu, Synthesis and biological evaluation of novel 2,4,5-substituted pyrimidine derivatives for anticancer activity, Bioorg. Med. Chem. Lett 19 (2009) 275–278, https://doi.org/10.1016/j.bmcl.2008.09.067.
[36] A. Matsuda, T. Sasaki, Antitumor activity of sugar-modified cytosine nucleosides, Cancer Sci. 95 (2004) 105–111, https://doi.org/10.1111/j.1349-7006.2004.tb03189.x.
[37] M.M. Mohamed, A.K. Khalil, E.M. Abbass, A.M. El-Naggar, Design, synthesis of new pyrimidine derivatives as anticancer and antimicrobial agents, Synth. Commun. 47 (2017) 1441–1457, https://doi.org/10.1080/00397911.2017.1332223.
[38] B. Testa, Prodrugs: bridging pharmacodynamic/pharmacokinetic gaps, Curr. Opin. Chem. Biol. 13 (2009) 338–344, https://doi.org/10.1016/j.cbpa.2009.04.620.
[39] R.H.J. Mathijssen, A. Sparreboom, J. Verweij, Determining the optimal dose in the development of anticancer agents, Nat. Rev. Clin. Oncol. 11 (2014) 272–281, https://doi.org/10.1038/nrclinonc.2014.40.
[40] S.T. Parvathy, V. Udayasuriyan, V. Bhadana, Codon usage bias, Mol. Biol. Rep. 49 (2022) 539–565, https://doi.org/10.1007/s11033-021-06749-4.
[41] V.P. Mauro, Codon optimization in the production of recombinant biotherapeutics: potential risks and considerations, BioDrugs 32 (2018) 69–81, https://doi.org/10.1007/s40259-018-0261-x.
[42] S. Inouye, Y. Sahara-Miura, J. Sato, T. Suzuki, Codon optimization of genes for efficient protein expression in Mammalian cells by selection of only preferred human codons, Protein Expr. Purif. 109 (2015) 47–54, https://doi.org/10.1016/j.pep.2015.02.002.
[43] P. Cano-Soldado, M. Pastor-Anglada, Transporters that translocate nucleosides and structural similar drugs: structural requirements for substrate recognition, Med. Res. Rev. 32 (2012) 428–457, https://doi.org/10.1002/med.20221.
[44] T. Fukami, T. Yokoi, The emerging role of human esterases, Drug Metabol. Pharmacokinet. 27 (2012) 466–477, https://doi.org/10.2133/dmpk.DMPK-12-RV-042.
[45] C. Grabbe, L. Cai, Regioselective deacetylation in nucleosides and derivatives, Chembiochem 25 (2024) e202400360, https://doi.org/10.1002/cbic.202400360.
[46] S. Azwar, H.F. Seow, M. Abdullah, M. Faisal Jabar, N. Mohtarrudin, Recent updates on mechanisms of resistance to 5-Fluorouracil and reversal strategies in Colon cancer treatment, Biology 10 (2021) 854, https://doi.org/10.3390/biology10090854.
[47] S.S.K. Yalamarty, N. Filipczak, X. Li, M.A. Subhan, F. Parveen, J.A. Ataide, et al., Mechanisms of resistance and current treatment options for glioblastoma multiforme (GBM), Cancers 15 (2023) 2116, https://doi.org/10.3390/cancers15072116.
[48] N. Urbelienė, S. Kutanovas, R. Meškienė, R. Gasparavičiūtė, D. Tauraitė, M. Koplūnaitė, et al., Application of the uridine auxotrophic host and synthetic nucleosides for a rapid selection of hydrolases from metagenomic libraries, Microb. Biotechnol. 12 (2019) 148–160, https://doi.org/10.1111/1751-7915.13316.